Plant Physiology®

Plant Physiology, 2025, **197**, kiaf067
https://doi.org/10.1093/plphys/kiaf067
Advance access publication 20 February 2025
Research Article

A powdery mildew core effector protein targets the host endosome tethering complexes HOPS and CORVET in barley

Björn Sabelleck,[1,2,†] Sohini Deb,[2,†] Sophie C.J. Levecque,[1] Matthias Freh,[1] Anja Reinstädler,[1] Pietro D. Spanu,[3] Hans Thordal-Christensen,[2,*] Ralph Panstruga[1,*]

[1]Institute for Biology I, Unit of Plant Molecular Cell Biology, RWTH Aachen University, Aachen 52056, Germany
[2]Department of Plant and Environmental Sciences, Section for Plant and Soil Sciences, University of Copenhagen, Frederiksberg C 1871 Denmark
[3]Department of Life Sciences, Imperial College London, Imperial College Road, London SW7 2AZ, UK
*Author for correspondence: htc@plen.ku.dk (H.T.-C.), panstruga@bio1.rwth-aachen.de (R.P.)
[†]These authors contributed equally to this work.
The author responsible for distribution of materials integral to the findings presented in this article in accordance with the policy described in the Instructions for Authors (https://academic.oup.com/plphys/pages/General-Instructions) is Ralph Panstruga.

Abstract
Powdery mildew fungi are serious pathogens affecting many plant species. Their genomes encode extensive repertoires of secreted effector proteins that suppress host immunity. Here, we revised and analyzed the candidate secreted effector protein (CSEP) effectome of the powdery mildew fungus, *Blumeria hordei* (*Bh*). We identified seven putative effectors that are broadly conserved in powdery mildew species, suggesting that they are core effectors of these phytopathogens. We showed that one of these effectors, CSEP0214, interacts with the barley (*Hordeum vulgare*) vacuolar protein-sorting 18 (VPS18) protein, a shared component of the class C core vacuole/endosome tethering (CORVET) and homotypic fusion and protein-sorting (HOPS) endosomal tethering complexes that mediate fusion of early endosomes and multivesicular bodies, respectively, with the central vacuole. Overexpression of CSEP0214 and knockdown of either *VPS18*, HOPS-specific *VPS41*, or CORVET-specific *VPS8* blocked the vacuolar pathway and the accumulation of the fluorescent vacuolar marker protein (SP)-RFP-AFVY in the endoplasmic reticulum. Moreover, CSEP0214 inhibited the interaction between VPS18 and VPS16, which are both shared components of CORVET as well as HOPS. Additionally, introducing CSEP0214 into barley leaf cells blocked the hypersensitive cell death response associated with resistance gene-mediated immunity, indicating that endomembrane trafficking is required for this process. CSEP0214 expression also prevented callose deposition in cell wall appositions at attack sites and encasements of fungal infection structures. Our results indicate that the powdery mildew core effector CSEP0214 is an essential suppressor of plant immunity.

Introduction

The powdery mildew fungi are obligate biotrophic pathogens belonging to the phylum Ascomycota and comprise ~900 species, which can infect nearly 10,000 species of angiosperm plants (Braun and Cook 2012). In the course of the infection, powdery mildew fungi secrete up to hundreds of effector proteins into the apoplastic space and the host cytosol to suppress plant defense responses and to manipulate the host cell metabolism for the benefit of the pathogen (Barsoum et al. 2019).

The powdery mildew pathogen, *Blumeria hordei* (*Bh*, formerly known as *B. graminis* f.sp. *hordei*; Liu et al. 2021), causing disease on barley (*Hordeum vulgare*), can lead to substantial yield losses in the field. Its unusually large genome codes for around 800 secreted proteins many of which are thought to act as effectors to promote pathogen virulence (Frantzeskakis et al. 2018). Of these, only few have been functionally characterized so far (Zhang et al. 2012; Pliego et al. 2013; Schmidt et al. 2014; Ahmed et al. 2015, 2016; Aguilar et al. 2016; Pennington et al. 2019; Li et al. 2021; Yuan et al. 2021; Liao et al. 2023; Li et al. 2024).

Upon recognition of fungal molecular structures, the plant immune system is activated in discrete steps (Jones and Dangl 2006), involving pattern-triggered immunity (PTI) and effector-triggered immunity (ETI) (Thordal-Christensen 2020). PTI comprises complex transcriptional reprogramming and cellular responses, including the deposition of cell wall appositions (papillae) at the sites of attack and the formation of encasements in the form of cell wall extensions that enclose pathogen structures (haustoria) invading the plant cell (Underwood 2012). As a countermeasure, the pathogen secretes effector proteins into the plant cytosol and apoplastic space to dampen and/or delay PTI.

Several *Arabidopsis thaliana* proteins are important for preinvasive immunity toward the nonadapted pathogen *Bh*, including the

Received July 23, 2024. Accepted December 31, 2024.
© The Author(s) 2025. Published by Oxford University Press on behalf of American Society of Plant Biologists.
This is an Open Access article distributed under the terms of the Creative Commons Attribution-NonCommercial-NoDerivs licence (https://creativecommons.org/licenses/by-nc-nd/4.0/), which permits non-commercial reproduction and distribution of the work, in any medium, provided the original work is not altered or transformed in any way, and that the work is properly cited. For commercial re-use, please contact reprints@oup.com for reprints and translation rights for reprints. All other permissions can be obtained through our RightsLink service via the Permissions link on the article page on our site—for further information please contact journals.permissions@oup.com.

Downloaded from https://academic.oup.com/plphys/article/197/4/kiaf067/8026087 by Bibliothek der RWTH Aachen user on 09 February 2026

PENETRATION (PEN) proteins (Underwood and Somerville 2008). The target membrane-associated soluble *N*-ethylmaleimide-sensitive-factor attachment receptor (t-SNARE, also referred to as syntaxin) SYNTAXIN of PLANTS121 (SYP121; synonym PEN1) is a component of an evolutionarily conserved defense pathway that relies on secretory processes (Rubiato et al. 2022). PEN1 and its putative orthologue in barley, REQUIRED FOR *mlo*-SPECIFIED RESISTANCE2 (ROR2), are required for papilla and encasement formation, probably by conferring fusion of multivesicular bodies (MVBs) to the plasma membrane (PM) at the site of fungal attack. Hereby, MVB intraluminal vesicles are secreted as extracellular vesicles (EVs) toward papillae and encasements, which are labeled with PEN1 or ROR2 (Collins et al. 2003; Assaad et al. 2004; Meyer et al. 2009; Böhlenius et al. 2010; Nielsen et al. 2012, 2017; Rubiato et al. 2022; Ruf et al. 2022).

Transport along the endomembrane trafficking pathway requires membrane fusion events involving early and late endosomes. In addition to SNARE proteins, this process needs endosomal tethering factors, e.g. the class C "core vacuole/endosome tethering" (CORVET) complex that interacts with Rab5 GTPases, as well as the "homotypic fusion and protein-sorting" (HOPS) complex interacting with Rab7 GTPases (Takemoto et al. 2018). The CORVET and HOPS complexes share the class C vacuolar protein-sorting (Vps) complex, made up of VPS11, VPS16, VPS18, and VPS33. In addition, CORVET involves VPS3 and VPS8, while HOPS involves VPS39 and VPS41 (Rieder and Emr 1997; Peterson and Emr 2001). Maturation of early endosomes to late endosomes, which eventually fuse with the vacuole, requires switches from the CORVET to the HOPS complex and from Rab5 to Rab7 (Rink et al. 2005).

Here, we show that the *Bh* candidate effector CSEP0214, a highly conserved effector protein within the powdery mildew fungal lineage, interacts with the CORVET and HOPS complex protein, VPS18. Interaction occurs via, but not only, the conserved CFEM (common in fungal extracellular membrane) domain in CSEP0214 and the RING (really interesting new gene) domain of VPS18. We demonstrate that transient expression of CSEP0214 in barley epidermal cells perturbs the endomembrane trafficking pathway to the vacuole. This results in the sequestration of marker proteins in the endoplasmic reticulum (ER), thereby preventing transport to their destinations. Importantly, the presence of CSEP0214 hampers encasement formation as well as the *Mla1*- and *Mla3*-mediated hypersensitive response (HR) in response to *Bh* challenge, confirming that endomembrane trafficking is essential for both PTI and ETI in the course of the barley-powdery mildew interaction. We finally observe that CSEP0214 prevents interaction between VPS18 and VPS16, another CORVET/HOPS protein, providing mechanistic insight into how CSEP0214 may suppress endomembrane trafficking.

Results

In silico analysis of the *B. hordei* secretome and the definition of a core effectome of powdery mildew fungi

The first in-depth analysis of the *Bh* "candidate secreted effector proteins" (CSEPs) was performed more than a decade ago (Pedersen et al. 2012). Substantial advances during the last 10 years in algorithms, prediction tools and computer power, the accessibility of new large data sets (e.g. transcriptomics and proteomics; Bindschedler et al. 2016), and the release of an improved *Bh* genome assembly (Frantzeskakis et al. 2018), justify an updated survey of this group of proteins. Here, we aimed to provide a comprehensive summary and detailed in silico analysis of the entire *Bh* secretome, which includes an assignment of revised gene identifiers to CSEP numbers, the integration of published transcriptomics data, functional, and structural predictions with InterPro, Phyre[2], and Alphafold2, and the use of general prediction tools like EffectorP and Localizer (see Materials and Methods for details).

The definition of effector proteins in eukaryotic pathogens (including fungi) is rather arbitrary and has been widely debated in the past, but typically assumes the presence of an amino-terminal signal peptide (SP) for secretion and the absence of detectable transmembrane domains (Sonah et al. 2016). Based on these criteria, we performed the present computational analysis with an updated list of 800 *Bh* proteins predicted to be secreted (Frantzeskakis et al. 2018) to reduce the risk of missing out on any potential effector candidates. According to the EffectorP 3.0 prediction, 527 of these 800 proteins were classified as bona fide effector candidates (328 cytoplasmic, 96 apoplastic, and 103 cytoplasmic/apoplastic). This includes all known avirulence proteins of *Bh* and most CSEPs with identified plant targets. InterPro detected known domains in 266 of the 800 secreted proteins, whereby ribonuclease (IPR016191; 78 hits), protease/peptidase (various InterPro domains; 27 hits), and Egh16-like virulence factor (IPR021476; 23 hits) were the most prevalent assignments (Supplementary Table S1).

So far, only the core effectome of members of the *Blumeria* lineage, which infect grasses, was determined (Frantzeskakis et al. 2018); the core effectome of the entirety of monocot- and dicot-infecting powdery mildew fungi has not been studied. With this aim, we followed the bioinformatic strategy outlined in Fig. 1. We used the predicted 800-protein secretome of *Bh*, which has one of the best annotated powdery mildew fungal genomes, as a query for sequence-based searches against 17 genomes of 15 additional powdery mildew fungi covering a broad range of the powdery mildew species diversity (Fig. 1). Apart from the two grass-infecting *Blumeria* species, these fungi infect dicotyledonous host species, while no known powdery mildew fungi appear to infect non-grass monocots (Vaghefi et al. 2022). We performed TBLASTN searches with a relaxed e-value threshold of e^{-10} not to miss detection of any potential effector candidates in these *Bh* relatives. To account for incomplete and/or low quality genome sequences, we accepted candidate effectors that are present in the genomes of just 15 out of the 16 tested species. Based on these criteria, we detected 196 *Bh* sequences (Supplementary Table S2) that are conserved in the tested powdery mildew fungi. Among the remaining 604 proteins present in fewer than 15 powdery mildew genomes, 30 were exclusively present in *Bh*, suggesting they are species-specific effector proteins of the barley pathogen. To eliminate secreted housekeeping proteins and other conserved secreted proteins from the list of the 196 secreted proteins conserved in at least 15 out of the 16 tested powdery mildew species, TBLASTN searches were carried out with the *Bh* versions of those as queries against a selection of genomes of nonphytopathogenic ascomycete fungi (*Aspergillus* spp., *Penicillium* spp., and *Saccharomyces* spp.). This resulted in 168 secreted proteins that can be considered as common fungal housekeeping proteins. A TBLASTN search was performed with the remaining 28 proteins against the genomes of 23 other phytopathogenic Ascomycota (see legend of Fig. 1) to explore a potential overlap of effector sets. This ultimately resulted in seven proteins

Downloaded from https://academic.oup.com/plphys/article/197/4/kiaf067/8026087 by Bibliothek der RWTH Aachen user on 09 February 2026

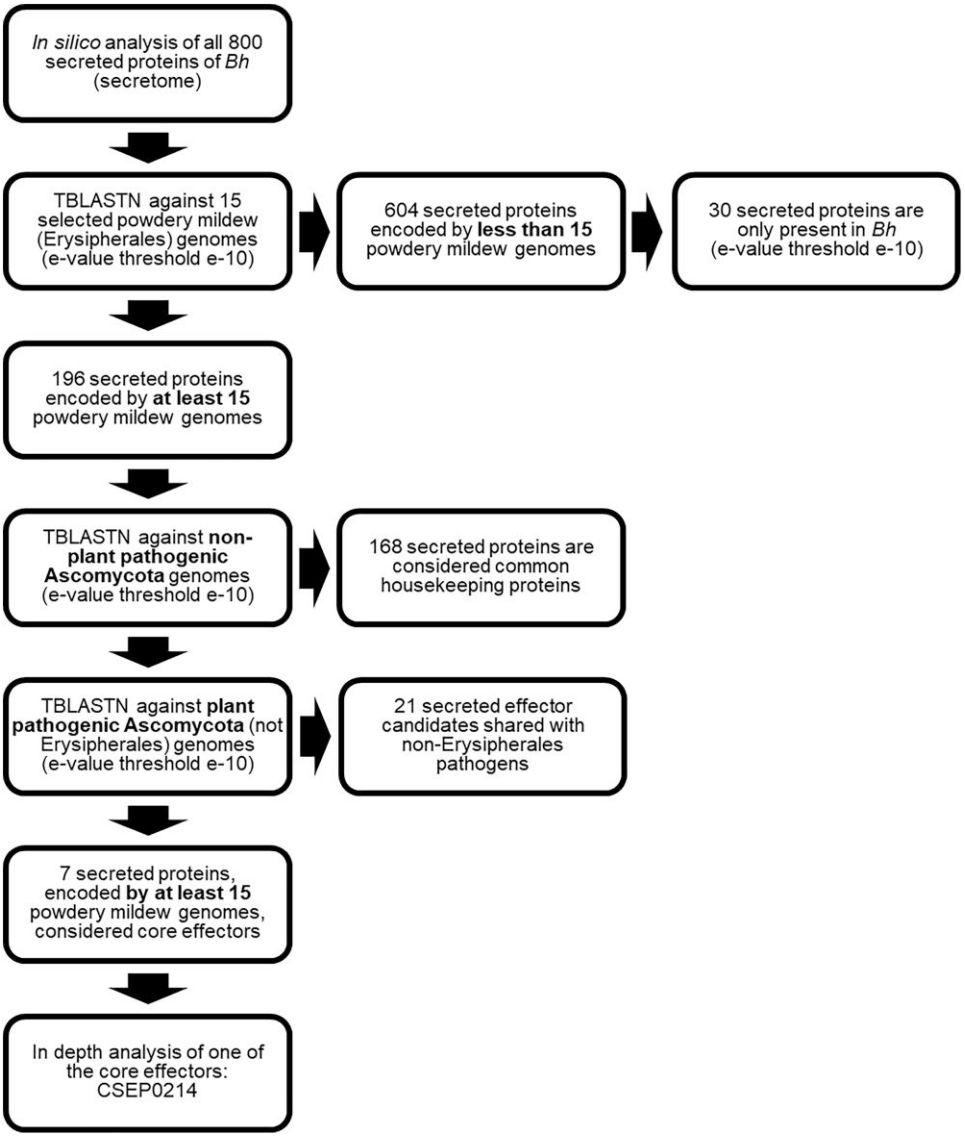


Figure 1. In silico analysis of the *B. hordei* (*Bh*) secretome and identification of the powdery mildew-specific core effectome. All 800 proteins of *Bh* that are predicted to be secreted were analyzed in silico (see Supplementary File S1 and Table S1) to obtain information on conserved domains and potential protein functions. TBLASTN searches were performed for these 800 *Bh* amino acid sequences against 17 genomes of 15 species from diverse phylogenetic clades of the *Erysiphaceae* (*B. graminis* f.sp. *triticale*, *B. graminis* f.sp. *tritici*, *Erysiphe alphitoides*, *E. necator*, *E. neolycopersici*, *E. pisi*, *Golovinomyces cichoracearum*, *G. magnicellulatus*, *G. orontii*, *Leveillula taurica*, *Parauncinula polyspora*, *Phyllactinia moricola*, *Pleochaeta shiraiana*, *Podosphaera leucotricha*, and *P. xanthii*). The 196 sequences found to be conserved in at least 15 out of the 16 genomes at an e-value threshold e^{-10} were searched by TBLASTN against three nonplant pathogenic ascomycetes (*Aspergillus* spp., *Penicillium* spp., and *Saccharomyces* spp.), which identified 168 common potential fungal housekeeping proteins. The remaining 28 sequences were used for TBLASTN searches against a selection of plant-pathogenic ascomycetes (*Alternaria* spp., *Bipolaris* spp., *Botrytis* spp., *Claviceps* spp., *Colletotrichum* spp., *Curvularia* spp., *Drechslera* spp., *Drepanopeziza* spp., *Exserohilum* spp., *Fusarium* spp., *Gaeumannomyces* spp., *Magnaporthe* spp., *Monilinia* spp., *Pyrenophora* spp., *Pyricularia* spp., *Ramularia* spp., *Rhynchosporium* spp., *Sclerotinia* spp., *Septoria* spp., *Thielaviopsis* spp., *Venturia* spp., *Verticillium* spp., and *Zymoseptoria* spp.) to define the core effectome specific for the powdery mildew fungi. This revealed seven putative effector proteins that are exclusively present and highly conserved within the powdery mildew fungi (respective genes present in the genomes of at least 15 of the 16 (including *Bh*) analyzed powdery mildew species; see also Supplementary Table S2).

that according to our analysis represent the conserved core effectome specific for the investigated powdery mildew fungi, while 21 proteins are also present in other plant-pathogenic fungi (Supplementary Table S2). One of the seven powdery mildew-specific core candidate effectors is CSEP0214 (*B. hordei* identifier BLGH_02334), a protein of 133 amino acids (including its amino-terminal SP), for which we provide a detailed in silico analysis, characterization of the interaction with its primary plant target, and an investigation of the cell biology and immunity-related phenotypes upon its expression in barley host cells.

CSEP0214 encodes a CFEM domain-containing protein and is highly expressed during fungal pathogenesis

The initial analysis described above, as well as TBLASTN searches in other powdery mildew fungal genomes, revealed that genes closely related to *Bh CSEP0214* are present in most of the tested powdery mildew fungal genomes, except in the early diverged and thus distantly related *P. polyspora*. We also failed to detect a CSEP0214 homolog in *Arachnopeziza araneosa*, a saprophyte that is the closest known relative of the powdery mildew fungi

Downloaded from https://academic.oup.com/plphys/article/197/4/kiaf067/8026087 by Bibliothek der RWTH Aachen user on 09 February 2026

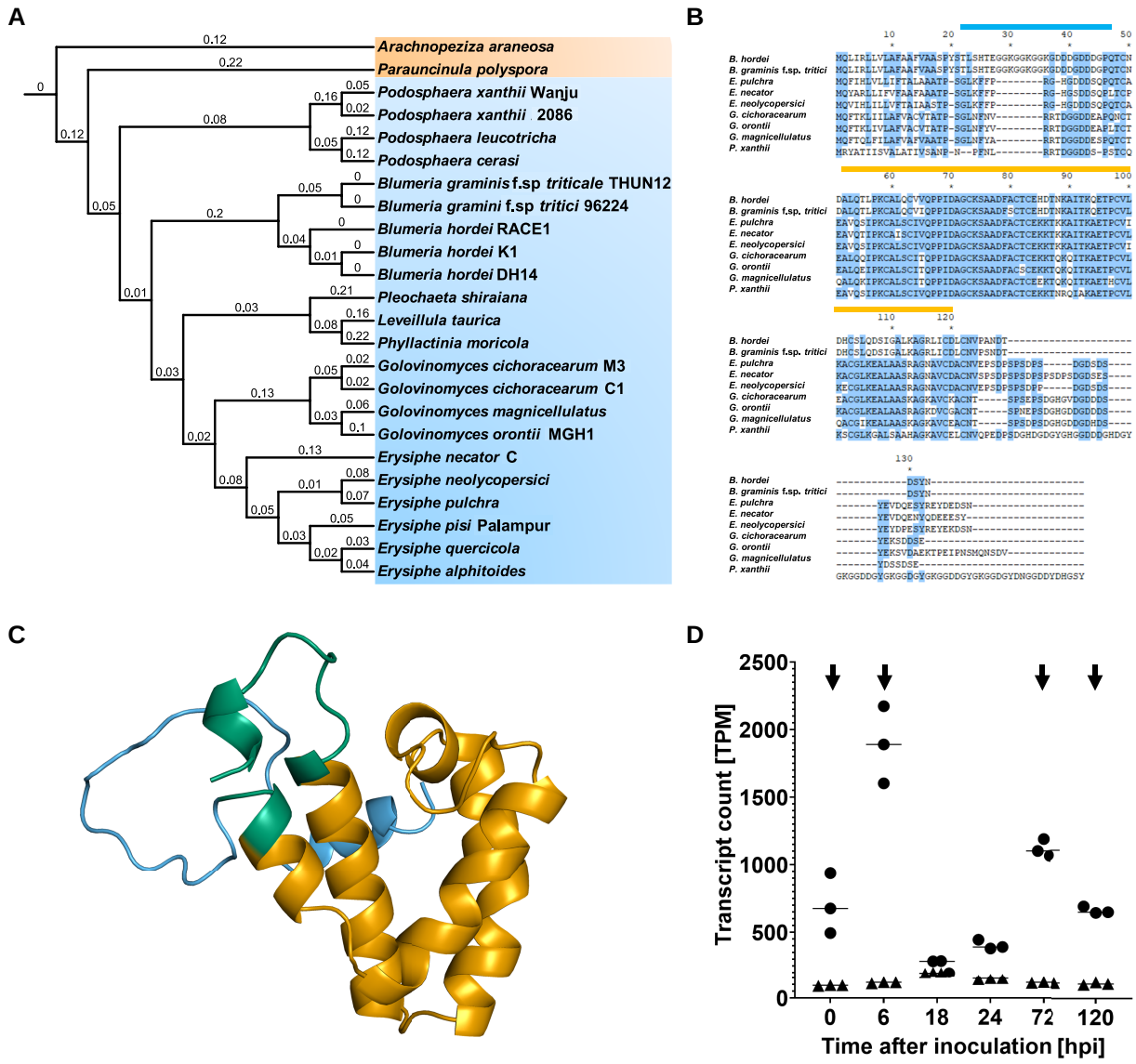


Figure 2. In silico analysis of *B. hordei* CSEP0214. **A)** Phylogenetic tree (cladogram) of powdery mildew fungi based on the amino acid sequences of 129 homologs single copy proteins (Vaghefi et al. 2022). Numbers at branches refer to the average frequency of amino acid substitutions per site. Fungi with CSEP0214 homologs are shown in blue, fungi lacking CSEP0214 are depicted in orange. **B)** Amino acid alignment of CSEP0214 homologs of nine powdery mildew species. Conserved amino acids (i.e. present in >55% of the sequences) are marked in blue. The blue bar above the alignment specifies the predicted disordered region and the orange bar indicates the predicted CFEM domain. **C)** Alphafold2-based prediction of the CSEP0214 3D structure; the predicted CFEM domain (orange) and the disordered region (light blue) as predicted by InterPro (https://www.ebi.ac.uk/interpro/search/sequence/) are highlighted. The protein regions outside these two domains are shown in turquoise. **D)** Expression levels of *CSEP0214* (circles) in TPM based on three independent replicates of a time-course infection experiment of *Bh* isolate K1 on the susceptible barley cv. Margret compared to the average expression of transcripts of all 800 predicted secreted *Bh* proteins (triangles) at 0, 6, 18, 24, 72, and 120 h post inoculation (hpi). Bars indicate medians of $n = 3$ independent experiments. Arrows highlight time points where *CSEP0214* belongs to the top 30 expressed genes encoding secreted proteins. Whole transcriptome shotgun sequencing (RNA-Seq) data were retrieved from a previous study (Qian et al. 2023).

(Vaghefi et al. 2022; Fig. 2A). The amino acid alignment of CSEP0214 homologs revealed a high sequence conservation (49% to 80% identity) within the powdery mildew fungi (Fig. 2B). Among four *Bh* isolates of different geographical origin (A6 (Denmark), DH14 (UK), K1 (Germany), and RACE1 (Japan)), the predicted amino acid sequence was homomorphic, indicating low within-species diversity of this candidate effector.

We predicted functional protein domains in CSEP0214 with InterPro (Blum et al. 2021) and detected an amino-terminal SP, comprising amino acids 1 to 17, followed by a predicted disordered region and a CFEM domain (Fig. 2B). A CFEM domain is a fungus-specific protein domain with eight highly conserved cysteine residues and a proposed role in pathogenicity (Kulkarni et al. 2003). The greatest sequence conservation between the CSEP0214 homologs of powdery mildew fungi resides within this region (Fig. 2B). Prediction of the 3D structure of CSEP0214 by Phyre[2] and Alphafold2 enabled us to localize the position of the CFEM domain, the disordered region and undefined regions within the molecule (Fig. 2C).

We used available (NCBI BioProject ID PRJNA835302; Qian et al. 2023) whole transcriptome shotgun sequencing (RNA-Seq) data to investigate the expression profile of *CSEP0214* during the infection of *Bh* on barley. In order to visualize the expression profile, we plotted the transcripts per million (TPM) of *CSEP0214* and the

Downloaded from https://academic.oup.com/plphys/article/197/4/kiaf067/8026087 by Bibliothek der RWTH Aachen user on 09 February 2026

averaged TPM values of the transcripts of all proteins predicted to be secreted (800 proteins in total). This analysis revealed that the *CSEP0214* transcript accumulates biphasically at levels that are substantially higher than the average of the genes encoding secreted proteins. At 6 h post inoculation (hpi), around the time when the fungal appressorium is formed, the difference is around 18-fold, whereas it almost decreases to the averaged TPM level for all secreted proteins at 18 hpi. The transcript levels increase again at three days after inoculation, when there are secondary host cell penetration attempts (Fig. 2D). Overall, the *CSEP0214* transcript is among the 30 most abundant transcripts at both early (0 and 6 hpi) and late (72 and 120 hpi) time points during infection (Fig. 2D). Thus, we speculate that this profile ensures high levels of CSEP0214 are present coincident with fungal host cell penetration.

CSEP0214 interacts with the CORVET and HOPS complex component protein VPS18

To identify potential host target(s) of the mature full-length (FL) CSEP0214 (lacking the SP; note that all following experiments were conducted with this version of the effector), we performed a classical GAL4-based yeast two-hybrid (Y2H) cDNA library screen and found a carboxy-terminal fragment of the barley RING domain protein, VPS18, as the most promising potential interaction partner (Supplementary Table S3). We recovered this carboxy-terminal fragment in 11 out of the 48 yeast colonies obtained in the Y2H screen. Cells of these 11 colonies activated the *HIS*, *ADE*, and *lacZ* reporter genes and could grow on medium with up to 25 mM 3-amino-1,2,4-triazole (3-AT), indicating a strong protein–protein interaction (Supplementary Table S3). The shortest overlap encoded by the 11 prey clones covers VPS18 amino acids 842 to 992, which defines an interval required for the interaction with CSEP0214. This VPS18 carboxy-terminal 151-amino acid segment contains the complete RING domain of the protein. VPS18 is a shared component of the HOPS and CORVET complexes. The CORVET complex is essential for the homotypic fusion between early endosomes or the heterotypic fusion between early endosomes and late endosomes/MVBs, while the HOPS complex is essential for the fusion of late endosomes and vacuoles. Thus, CORVET and HOPS serve as tethering factors for Rab5 and Rab7 GTPases, respectively (Seals et al. 2000; Peplowska et al. 2007; Balderhaar and Ungermann 2013). For verification of the interaction between CSEP0214 and VPS18, we performed split-ubiquitin Y2H experiments with the 992-amino acid FL version of VPS18. Combining VPS18, translationally fused to Cub-PLV at its carboxy-terminus, with NubG-CSEP0214, resulted in yeast growth on interaction-selective medium (Fig. 3A), corroborating the CSEP0214-VPS18 interaction. The split-ubiquitin Y2H system rather than the conventional GAL4-based Y2H system was chosen for this experiment as FL VPS18 did not express well in the latter.

We further performed coimmunoprecipitation (co-IP) experiments to validate our yeast-based results. To this end, we transiently coexpressed fluorophore (mRFP or mCherry)-tagged FL VPS18 with hemagglutinin (HA)-tagged CSEP0214 (lacking its SP) or the respective empty vectors (EVs; as negative controls), in different combinations in leaves of *Nicotiana benthamiana* and used red fluorescent protein (RFP) trap beads to purify potential protein complexes from the respective plant lysates (Fig. 3B; Supplementary Fig. S1A). On the co-IP immunoblot probed with α-HA antibody, we observed a high-molecular mass band when HA-CSEP0214 was coexpressed with mRFP-VPS18, indicative of a highly stable VPS18-CSEP0214 complex that cannot be resolved under standard protein gel conditions. We did not observe any co-IP signal on the α-HA-probed immunoblot when we coexpressed mRFP-VPS18 and HA-CSEP0105, an unrelated *B. hordei* effector protein chosen as a negative control (Fig. 3B).

As a third independent approach to analyze the VPS18-CSEP0214 interaction, we conducted in planta luciferase complementation imaging experiments. In this assay, reconstitution of active firefly luciferase by interaction of NLuc- and CLuc-tagged bait and prey proteins gives rise to light emission that can be quantified (Chen et al. 2008). In *N. benthamiana* leaves, we transiently coexpressed either C- or N-terminally tagged versions of FL VPS18 with N-terminally tagged versions of CSEP0214 or two unrelated CSEPs (CSEP0051 and CSEP0061, which failed to interact with VPS18 in the GAL4-based Y2H assay; see below and Supplementary Fig. S2A) and quantitatively determined the respective light emission. The previously established interaction between MLO6-NLuc and CLuc-CAM2 (Huebbers et al. 2024) served as positive control and reference for normalization of the luminescence. We found that VPS18, either N- or C-terminally tagged with CLuc, yielded a very strong signal (>3-times the luminescence obtained for the MLO6-CAM2 reference and close to saturation of the detection system) when coexpressed with NLuc-CSEP0214, but neither with NLuc-CSEP0051 nor with NLuc-CSEP0061 (Fig. 3C and D). By contrast, all combinations tested for VPS18 N- or C-terminally tagged with NLuc failed to generate meaningful light emission. Immunoblot analysis revealed that this might be due to low accumulation of the NLuc-tagged VPS18 fusion proteins. Meanwhile, the three effectors tested (CSEP0051, CSEP0061, and CSEP0214) did not show any marked differences in detectable protein levels (Supplementary Fig. S1B). Taken together, three independent assays (split-ubiquitin Y2H, co-IP, and luciferase complementation imaging) provided strong evidence for an interaction between *Bh* CSEP0214 and FL barley VPS18.

We next tested if the interaction between CSEP0214 and VPS18 is specific. Therefore, we performed a GAL4-based Y2H experiment with the 151-amino acid RING domain fragment of VPS18, originally recovered in the Y2H screen (see above), against a test set of ten randomly selected *Bh* CSEPs. As judged from yeast growth on interaction-selective medium, and in contrast to CSEP0214, none of these CSEPs were able to interact with the VPS18 RING domain (Supplementary Fig. S2A). To demonstrate that a lack of interaction in the Y2H assay was not due to failed expression of the CSEPs, we performed immunoblot analysis and found that eight of the CSEPs were detectably expressed, albeit at different levels (Supplementary Fig. S2B). To explore whether CSEP0214 interacts specifically with the RING domain of VPS18, we tested the RING domains of barley PEX2 and PEX12 (see sequence alignment in Supplementary Fig. S2C), two barley peroxins involved in mediating peroxisomal protein import (Kao et al. 2016). Neither of these showed signs of interaction in the classical Y2H assay (Supplementary Fig. S2D).

We raised polyclonal peptide antibodies against two different regions of CSEP0214 (Supplementary Table S4) and affinity-purified them individually against the two peptides used for immunization (for details, see Materials and Methods). These purified antisera were tested using recombinant 6x-His-CSEP0214 protein inducibly expressed in *Escherichia coli*, and we detected a band corresponding to the molecular mass of CSEP0214 (~12 kDa) in bacterial lysates (Supplementary Fig. S3). The affinity-purified antiserum was subsequently used in immunoblots to analyze if we can detect CSEP0214 in protein samples from *Bh*-infected barley leaves. Besides unspecific binding products that were present in both non-inoculated and

Downloaded from https://academic.oup.com/plphys/article/197/4/kiaf067/8026087 by Bibliothek der RWTH Aachen user on 09 February 2026

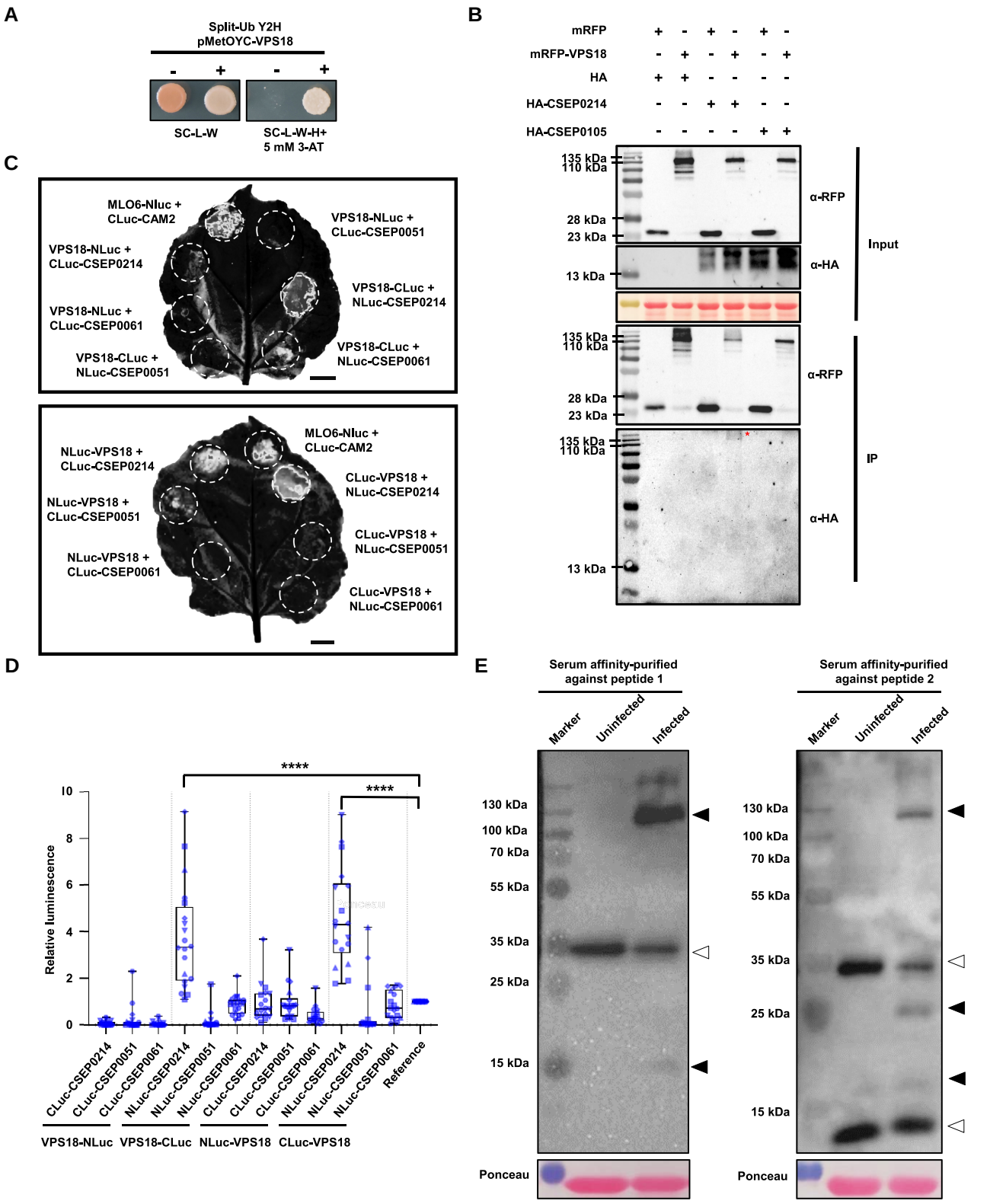


Figure 3. Interaction of CSEP0214 with VPS18. **A)** LexA-based split-ubiquitin Y2H assay of barley FL VPS18 expressed from vector pMetOYC (VPS18-Cub-PLV) and NubG-CSEP0214 (without SP) expressed from vector pNX32 (+) in the yeast strain THY.AP4. The empty pNX32 vector was used as negative control (–). Yeast growth on medium that is selective for the presence of the plasmids (SC-L-W; growth control) is shown on the left, and yeast growth on interaction-selective medium (SC-L-W-H+5 mM 3-AT) is shown on the right, after three days of growth. The experiment was performed four times with a similar outcome. **B)** Fusion proteins mCherry-VPS18, HA-CSEP0214, HA-CSEP0105, or the mCherry and HA tags alone were coexpressed in different combinations via *A. tumefaciens*-mediated transient gene expression in leaves of *N. benthamiana* plants. Proteins were extracted for co-IP. Protein samples of the IP and the total protein extract (Input) were used for SDS-PAGE and immunoblot analysis. The membranes were probed with α-RFP and α-HA antibodies, respectively. On the left, molecular masses of marker proteins are given. Ponceau staining was used to demonstrate equal amounts of total proteins on the blots. Note the presence of a high-molecular mass signal (>135 kDa) in the immunoblot probed with the α-HA antibody

(continued)

Downloaded from https://academic.oup.com/plphys/article/197/4/kiaf067/8026087 by Bibliothek der RWTH Aachen user on 09 February 2026

Bh-inoculated leaf samples, we detected a weak band (~15 kDa) corresponding approximately to the calculated molecular mass of CSEP0214 (~12 kDa) specifically in inoculated leaf samples. We further observed stronger bands of high-molecular mass (at ~130 kDa). These were likewise only present in samples from *Bh*-inoculated leaves and could correspond to a complex composed of the 992-amino acid VPS18 (~109 kDa) and CSEP0214 (Fig. 3E). Interestingly, the antibody raised and affinity-purified with peptide 2, covering part of the conserved CFEM domain, but not the one made with peptide 1, additionally detected a ~25 kDa-protein in the extract derived from *Bh*-challenged leaf tissue (Fig. 3E). This band potentially corresponds to a CSEP0214 dimer. Hence, we tested for the ability of CSEP0214 to interact with itself in a split-ubiquitin based Y2H, and indeed observed self-association of the effector (Supplementary Fig. S4).

Having found that CSEP0214 and VPS18 might form a stable complex in planta, we wanted to analyze the strength of this interaction in more detail. Therefore, we performed an immunoblot experiment using combinations of mCherry-VPS18 and 3xHA-CSEP0214 as well as EV controls expressed in leaves of *N. benthamiana*. The proteins were extracted using either a standard extraction buffer or a denaturation buffer containing high concentrations of urea and thiourea ("urea buffer"), and separated by sodium dodecyl sulfate-polyacrylamide gel electrophoresis (SDS-PAGE). On an anti-HA immunoblot, we detected an effector-specific band of <28 kDa. However, in the sample extracted with the mild buffer, and not with the denaturation buffer, we also detected a band of ~140 kDa using the anti-HA antibody (Supplementary Fig. S5). This outcome is indicative of a heat- and SDS-resistant VPS18-CSEP0214 complex that can only be dissolved by strong denaturing agents.

The C-terminal portion of the CFEM domain in CSEP0214 and the RING domain of VPS18 are essential for the interaction

To narrow down the potential interaction site within CSEP0214, we created seven truncated versions of the effector protein (Fig. 4A) and analyzed these for interaction with the RING domain of VPS18 GAL4-based Y2H experiments. Here, we only saw interaction when CSEP0214 amino acids 85 to 107 were included but not with the fragments located N-terminally hereof. Thus, $CSEP0214^{1–34}$, $CSEP0214^{1–71}$, $CSEP0214^{1–85}$, and $CSEP0214^{31–71}$ failed to interact with the VPS18 RING domain (Fig. 4B). To validate this result, we confirmed expression of the truncated CSEPs in the yeast strains by immunoblot-based detection of the GAL4-binding domain of the various constructs (Supplementary Fig. S6). However, when we tested FL CSEP0214 and truncations thereof with FL VPS18 in a split-ubiquitin Y2H, we observed surprisingly that FL CSEP0214 as well as all the truncated versions showed interaction with FL VPS18. These truncated variants included at least three essentially non-overlapping CSEP0214 domains ($CSEP0214^{1–34}$, $CSEP0214^{31–71}$, and $CSEP0214^{85–107}$), indicating that $CSEP0214^{1–84}$ may be involved in interaction with VPS18 in regions other than the RING domain (Supplementary Fig. S7). Altogether, the results suggest that the C-terminal region of the CFEM domain in CSEP0214 (between amino acids 85 and 107) is essential for the interaction with the VPS18 RING domain. However, the remaining part of CSEP0214 is likely involved in interaction with regions in VPS18 other than the RING domain. Confirming this in the split-ubiquitin Y2H system, we indeed saw interaction between VPS18 ΔRING (lacking the C-terminal region with the RING domain) and FL CSEP0214 (Fig. 4C and D; Supplementary Fig. S8). All-in-all, the studies suggest a complex interaction between the two proteins, involving at least three CSEP0214 and two VPS18 domains.

Expression of CSEP0214 in barley leaf epidermal cells or knockdown of its target perturbs the endomembrane trafficking pathway

As VPS18 is known to be a shared component of the CORVET and HOPS complexes involved in the vacuolar transport pathway (van der Kant et al. 2015), we wanted to examine if CSEP0214 affects this route via interaction with VPS18. Thus, we transiently expressed in barley leaf epidermal cells CSEP0214 lacking its SP and the vacuolar marker (SP)-RFP-AFVY, where the 4-amino acid vacuolar targeting signal of the vacuolar lumen protein, phaseolin (Hunter et al. 2007), was added to the C-terminus of RFP. We observed that expression of CSEP0214 caused a significant fraction of this vacuolar marker protein to be retained in an ER-like reticulate structure (Fig. 5A). The ER identity of this structure was confirmed by colocalization with a fluorescent luminal ER marker, (SP)-mYFP-HDEL (i.e. monomeric yellow fluorescent protein (YFP) with the carboxy-terminal HDEL ER retention signal; Irons et al. 2003) in 44 out of 50 cells studied, as compared to six out of 50 when CSEP0214 was not coexpressed, or eight out of 50 cells when CSEP0055 was coexpressed as a negative control (Fig. 5A).

To support that CSEP0214 acts via VPS18, we used an RNA interference (RNAi) approach targeting *VPS18* and *VPS41*. In these experiments, we bombarded barley leaf epidermal cells with RNAi constructs, designed for the knockdown of *VPS18* and *VPS41*, along with the vacuolar marker (SP)-RFP-AFVY. The *hrpE*

Figure 3. (Continued)
upon coexpression of mRFP-VPS18 and HA-CSEP0214. The experiment was performed four times with a similar outcome (see Supplementary Fig. S1A for another independent replicate). **C**, **D)** Fusion proteins CLuc-VPS18, VPS18-CLuc, NLuc-VPS18, or VPS18-NLuc were coexpressed with either NLuc- or CLuc-tagged CSEP0051, CSEP0061, or CSEP0214 via *A. tumefaciens*-mediated transient gene expression in leaves of *N. benthamiana* plants. D-Luciferin was applied three days after agroinfiltration and luminescence measured after incubation for 10 min in the dark. Samples for immunoblots were taken three days after agroinfiltration. **C)** Representative *N. benthamiana* pseudocolored leaves at three days after agroinfiltration. Lighter grayscales indicate a higher amount of luminescence. Images were digitally extracted for comparison. Scale bars, 1 cm. **D)** Quantitative analysis of relative luminescence in relation to the reference interaction of MLO6-NLuc and CLuc-CAM2 (Huebbers et al. 2024), set as 1 ("Reference"). Boxplots show the outcome of six experimental replicates with two to four data points per replicate, i.e. a minimum of 12 data points per combination. Different geometric symbols represent the data points of the individual replicates. Center lines show the medians; upper and lower box limits indicate the 25th and 75th percentiles respectively; upper and lower whiskers mark the highest and lowest values, respectively. ****, $P < 0.0001$; assessed by One-way ANOVA followed by Dunnett's multiple comparisons test. **E)** Immunoblot detection of CSEP0214 in total protein extracts of *Bh*-infected (5 dpi with virulent isolate K1) and uninfected barley cv. Lottie leaves. Two antisera, raised against two separate regions of CSEP0214 (peptide 1 and 2; see Materials and Methods for details) and affinity-purified against these peptides, were used. White arrowheads mark unspecific bands present in samples from both uninfected and infected leaves, black arrowheads mark bands that are detectable solely in samples from infected leaves. On the left, molecular masses of marker proteins are given. Ponceau staining was used to demonstrate equal amount of total proteins on the blots. The experiment was performed once.

Downloaded from https://academic.oup.com/plphys/article/197/4/kiaf067/8026087 by Bibliothek der RWTH Aachen user on 09 February 2026

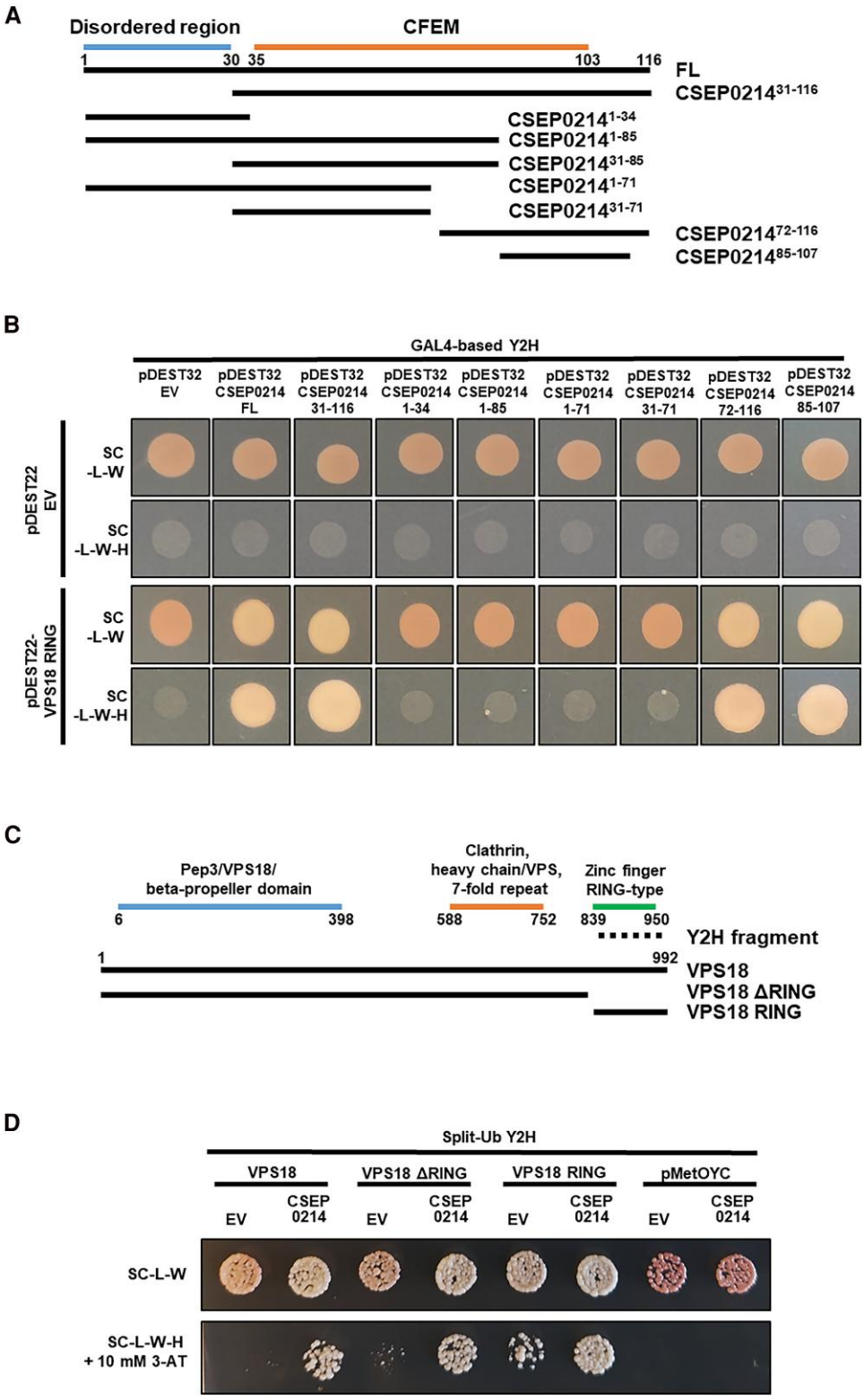


Figure 4. The C-terminal portion of the CFEM domain in CSEP0214 interacts with the VPS18 RING domain. **A)** Schematic representation of different truncated versions of CSEP0214 and indication of predicted domains. FL, full-length (without SP, 116 amino acids). The indicated numbering of the amino acids refers to this 116-aa version. **B)** GAL4-based Y2H assay of the VPS18 RING domain fused to the GAL4 activation domain was tested against truncations of CSEP0214 (see panel **A**) fused to the GAL4 binding domain. For the GAL4 binding domain fusion proteins, the EV (pDEST32) was used as negative control and CSEP0214 FL as positive control. For the GAL4 activation domain VPS18 RING fusion protein, the EV pDEST22 was used as negative control. Shown on the top of each panel is yeast growth on medium that is selective for the presence of the plasmids (-L-W; growth control). Shown on the bottom of each panel is yeast growth on interaction-selective medium (-L-W-H). The experiment was performed once. **C)** Schematic representation of VPS18 and two truncated versions (VPS18 ΔRING and VPS18 RING) and location of predicted domains. The numbering indicates the amino acid position of predicted domains. The dashed line depicts the fragment identified in the Y2H cDNA screen. **D)** LexA-based split-ubiquitin (Split-Ub) Y2H assay with FL and truncated versions of VPS18 expressed from pMetOYC (VPS18-Cub-PLV) and FL CSEP0214 expressed from pNX32 (NubG-CSEP0214). Images were taken after three days of growth. EV, empty vector. The experiment was performed three times with a similar outcome.

Downloaded from https://academic.oup.com/plphys/article/197/4/kiaf067/8026087 by Bibliothek der RWTH Aachen user on 09 February 2026

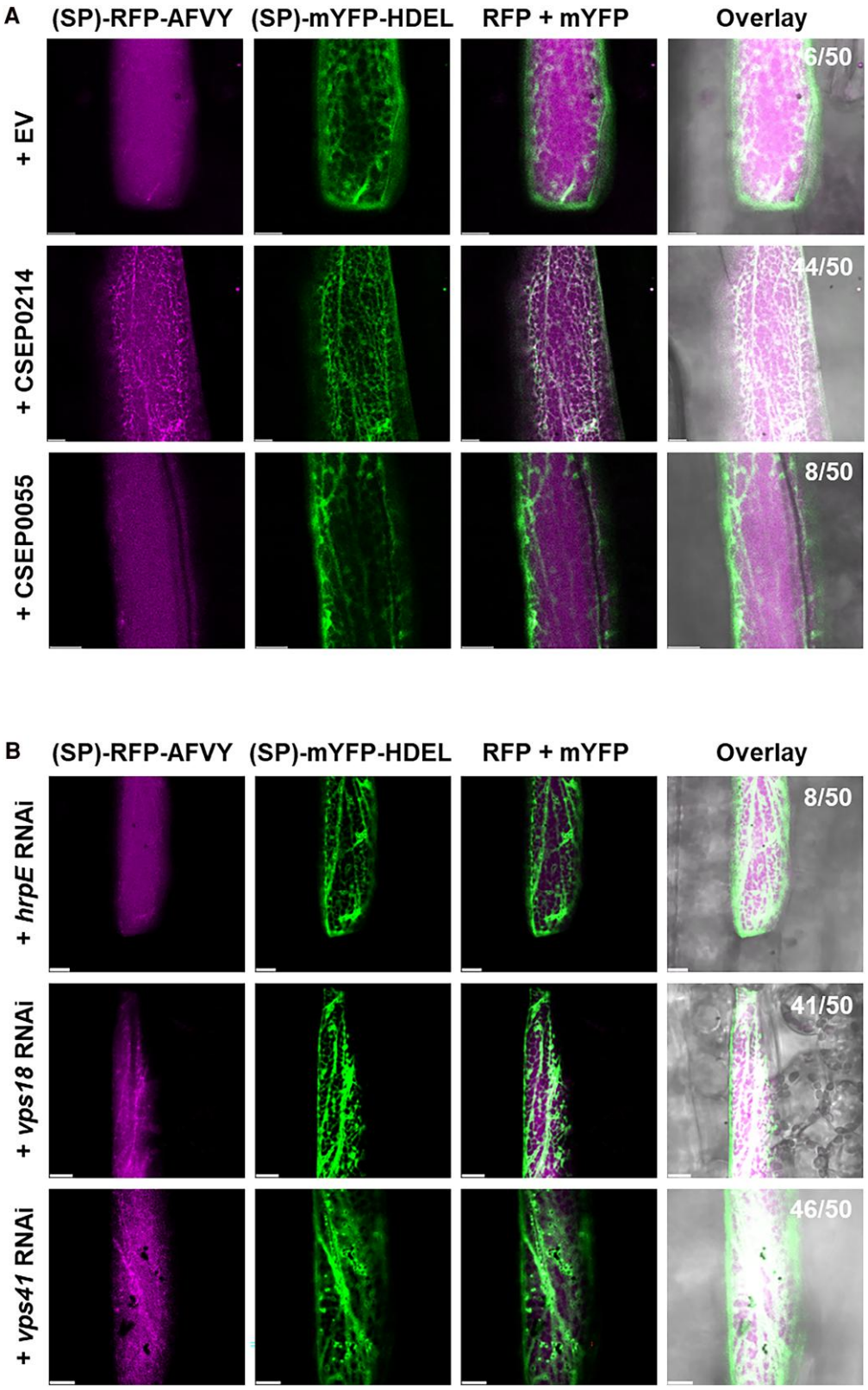


Figure 5. Expression of CSEP0214 in barley leaf epidermal cells or knockdown of the target blocks the transport of the vacuolar marker protein, (SP)-RFP-AFVY. Subcellular localization of the vacuolar marker (SP)-RFP-AFVY and the ER marker (SP)-mYFP-HDEL (SP, signal peptide) upon coexpression with either **A)** an EV (pUbi::GW), CSEP0214 (pUbi::CSEP0214), or CSEP0055 (pUbi::CSEP0055; used as negative control), or **B)** the *hrpE* control RNAi construct (pIPKTA30N::*hrpE*) or knockdown constructs of *VPS18* (pIPKTA30N::*VPS18*) and *VPS41* (pIPKTA30N::*VPS41*), in barley (cv. Golden Promise) by particle bombardment of leaf epidermal cells. Numbers in the top right corner of the overlay panels indicate the occurrence of colocalization with the (SP)-mYFP-HDEL ER marker in 50 inspected cells. Scale bar, 10 µm.

Downloaded from https://academic.oup.com/plphys/article/197/4/kiaf067/8026087 by Bibliothek der RWTH Aachen user on 09 February 2026

gene from the type-III secretion system of the bacterial phytopathogen *Pseudomonas syringae* was used as a nonplant RNAi control. We observed specifically that RNAi-based knockdown of *VPS18* or *VPS41* caused retention of the fluorescent vacuolar marker in reticulate structures that co-localized with the ER marker, (SP)-mYFP-HDEL, similar to the effect seen upon the overexpression of CSEP0214 (Fig. 5B). In order to further confirm this observation, we wanted to test if putative dominant-negative variants of VPS18 and VPS41 affected this route. Thus, we transiently expressed the RING domains, and the FL versions of these proteins as controls, along with the vacuolar marker, (SP)-RFP-AFVY, in barley leaf epidermal cells. In all four cases, this led to ER localization of the vacuolar marker (Supplementary Fig. S9). Expression of FL VPS18 or VPS41 also blocked (SP)-RFP-AFVY in the ER, indicating that correct stoichiometry of the components in the CORVET and/or HOPS complexes is essential for proper function in endomembrane trafficking (Supplementary Fig. S9). Moreover, RNAi of the CORVET-specific *VPS8* showed a similar block of (SP)-RFP-AFVY in the ER (Supplementary Fig. S10A).

In addition, expression of CSEP0214 resulted in a partial overlap between the fluorescent Golgi ST-YFP marker (a fusion of the 52-amino acid signal anchor of a rat sialyltransferase fused to YFP; Brandizzi et al. 2002) and the (SP)-mYFP-HDEL ER marker in 32 out of 50 cells studied, compared to none out of 50 in case of the EV control (Supplementary Fig. S12A). This indicates that CSEP0214 caused ST-YFP to be retained in the ER. Furthermore, CSEP0214 expression blocked the otherwise secreted protein marker, (SP)-mCherry, leading to its accumulation in intracellular aggregates and an ER-like structure (Supplementary Fig. S12B).

Expression of CSEP0214 in barley leaf epidermal cells or knockdown of its target blocks the transport and accumulation of the papilla marker protein, ROR2

In order to explore whether CSEP0214 affects a known immunity-associated endomembrane trafficking pathway, the transport of marker proteins upon *Bh* challenge to the papilla was examined. We coexpressed the established papilla marker, mCherry-ROR2 (Bhat et al. 2005), with CSEP0214 in barley leaf epidermal cells, followed by *Bh* inoculation. In the EV control, mCherry-ROR2 localized at the PM and in papillae formed at *Bh* attack sites (Fig. 6A). This strong mCherry-ROR2 labeling of extracellular papillae agrees with previous observations that this membrane protein and its orthologue, Arabidopsis PEN1, are markers for EVs (Meyer et al. 2009; Böhlenius et al. 2010; Nielsen et al. 2012). However, when coexpressed with CSEP0214, mCherry-ROR2 did not localize at papillae, but instead appeared in discrete structures, accumulating near the fungal attack site and to some extent in ER-like structures, in 46 out of 50 cells studied, compared to eight out of 50 in the EV control (Fig. 6A). In the absence of *Bh* challenge, CSEP0214 expression led to localization of ROR2 in a reticulate structure overlapping with the (SP)-mYFP-HDEL ER marker (Supplementary Fig. S12C). The observed effect of the CSEP0214-induced block of ROR2 transport to papillae could also be seen upon RNAi of *VPS18* or *VPS41* (Fig. 6B), or RNAi of *VPS8* (Supplementary Fig. S10B). Coexpression of either VPS18, VPS18-RING, VPS41, or VPS41-RING also blocked ROR2 localization to papillae, and mCherry-ROR2 was observed in an ER-like structure rather than in the papillae, indicating that these proteins are important for this cellular trafficking pathway (Supplementary Fig. S11).

CSEP0214 mediates susceptibility by blocking immune receptor-induced HR and the encasement of fungal infection structures

Previously, MON1, involved in the activation of the late endosome GTPase Rab7, has been found to be important for encasement formation and the HR in response to powdery mildew fungi in barley and *A. thaliana* (Liao et al. 2023). Since we provide data above indicating that CSEP0214 affects HOPS, the tethering complex of Rab7, we analyzed whether CSEP0214 hampered these immune responses as well. To test for the occurrence of HR, we used the barley lines P01 and P02, which are immune to *Bh* isolates C15 and A6, respectively. The isolate-specific immunity in these lines is mediated by the allelic *Mla1* (P01) and *Mla3* (P02) resistance genes, encoding coiled-coil, nucleotide-binding, leucine-rich repeat (CNL)-type resistance proteins (Kølster et al. 1986; Seeholzer et al. 2010). We used the bacterial *Pseudomonas fluorescence* strain EtHAn, engineered to express a *P. syringae* type 3-secretion system, and the pEDV6 vector (Thomas et al. 2009; Fabro et al. 2011), to introduce either β-glucuronidase (GUS, control; Li et al. 2024), or CSEP0214 into leaf cells of barley lines P01 or P02 by infiltrating the bacteria into the leaf apoplastic space. The leaves were subsequently inoculated with the avirulent *Bh* isolates, C15 and A6, respectively. Samples were collected four days after infiltration/inoculation and stained with either Coomassie blue (Fig. 7A, C, E, and G) to visualize fungal hyphae, or with trypan blue (Fig. 7B, D, F, and H) to detect host cell death. Pathogenic growth of the fungus was significantly increased, quantified as secondary hyphal growth and conidiophore production, after delivery of CSEP0214 (Fig. 7I and J). In addition, CSEP0214 suppressed the HR-like cell death in these otherwise resistant barley lines (Fig. 7K).

We next analyzed the extent of callose deposition in papillae upon transient expression of CSEP0214. Either EV or a construct for expression of untagged CSEP0214 were introduced into barley leaf epidermal cells by particle bombardment along with a construct expressing β-GUS to allow the detection of transformed cells. In this assay, we observed a significant reduction in callose deposition in papillae following expression of CSEP0214 in the leaf cells (Fig. 7L). *Bh* normally does not induce encasement formation in barley. However, this immune-related structure is formed when the plants are sprayed with the fungicide, tetraconazole (Maffi et al. 1995; Liao et al. 2023). The formation of tetraconazole-induced encasements was significantly reduced following CSEP0214 expression (Fig. 7M). To analyze whether the reduced callose response affected the fungal host cell entry rate, we introduced constructs for expression of CSEP0214, VPS18, and the VPS18 RING domain by particle bombardment. None of the three constructs caused a statistically significant difference from the EV control regarding the rate of haustorium formation (Supplementary Fig. S13).

Expression of CSEP0214 inhibits interaction of VPS18 with VPS16

In order to investigate further how CSEP0214 inhibits the function of VPS18, we wanted to analyze if CSEP0214 inhibits the interaction between VPS18 and VPS16, another component of the CORVET and HOPS complex. These two proteins have earlier been shown to associate (Graham et al. 2013; van der Kant et al. 2015; Shvarev et al. 2022). We performed split-ubiquitin Y2H experiments with VPS18 (FL), fused to Cub-PLV (pMetOYC), against VPS16 (FL)-NubG (pXN22). When coexpressed with EV (pAG426-GPD-GW; Alberti et al. 2007), we observed yeast growth

Downloaded from https://academic.oup.com/plphys/article/197/4/kiaf067/8026087 by Bibliothek der RWTH Aachen user on 09 February 2026

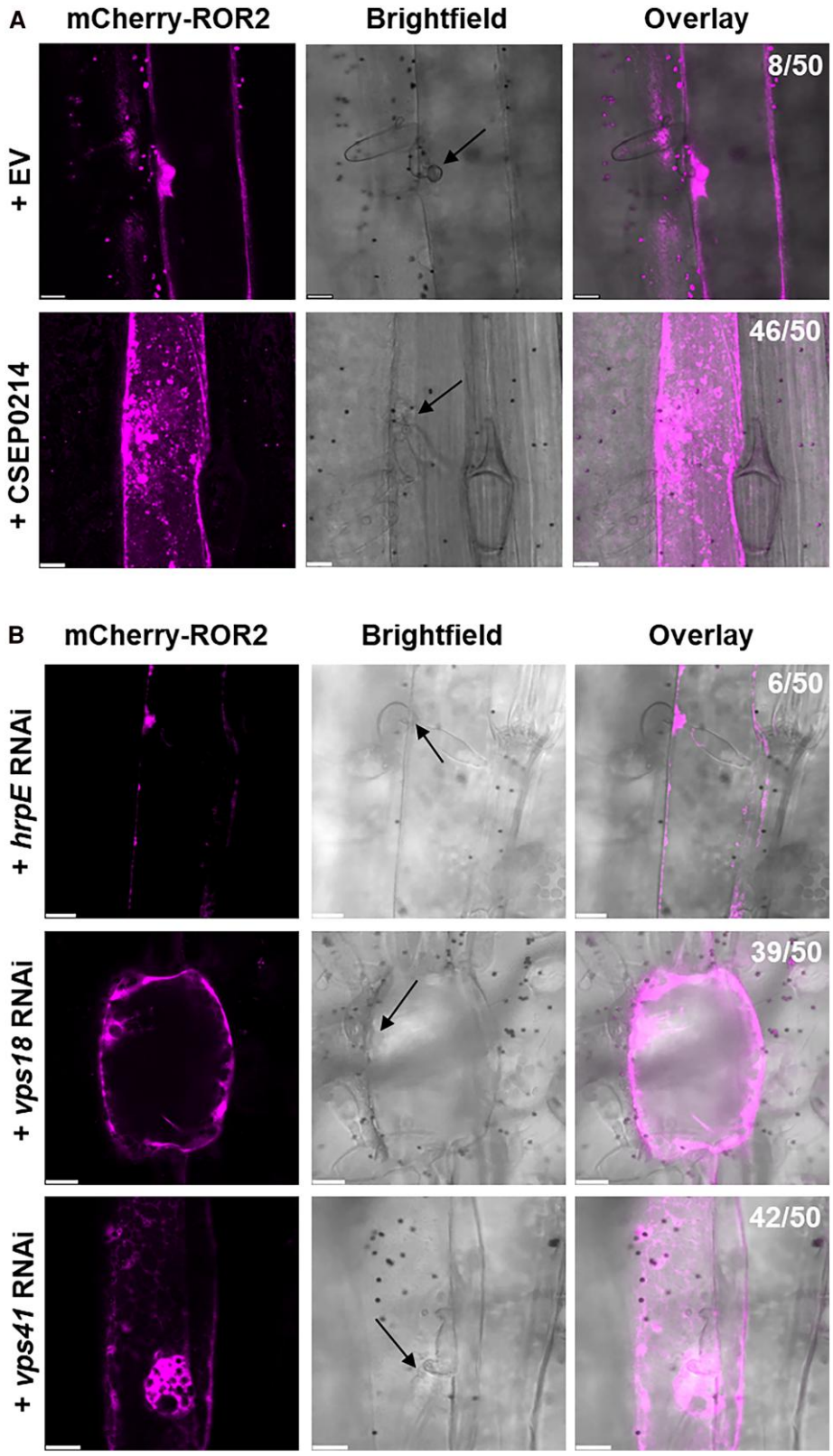


Figure 6. Expression of CSEP0214 in barley leaf epidermal cells or knockdown of the target blocks the transport and accumulation of the papilla marker protein, ROR2. Subcellular localization of the papilla marker mCherry-ROR2 upon coexpression with either **A)** an EV (pUbi::GW) or CSEP0214 (pUbi::CSEP0214), or **B)** the *hrpE* control RNAi construct (pIPKTA30N::*hrpE*) or RNAi constructs directed against *VPS18* (pIPKTA30N::*VPS18*) and *VPS41* (pIPKTA30N::*VPS41*), in barley (cv. Golden Promise) by particle bombardment of leaf epidermal cells. Arrows indicate fungal attack sites. Numbers in the top right corner of the overlay panels indicate the occurrence of unusual marker localization in 50 inspected cells. Scale bar, 10 µm.

Downloaded from https://academic.oup.com/plphys/article/197/4/kiaf067/8026087 by Bibliothek der RWTH Aachen user on 09 February 2026

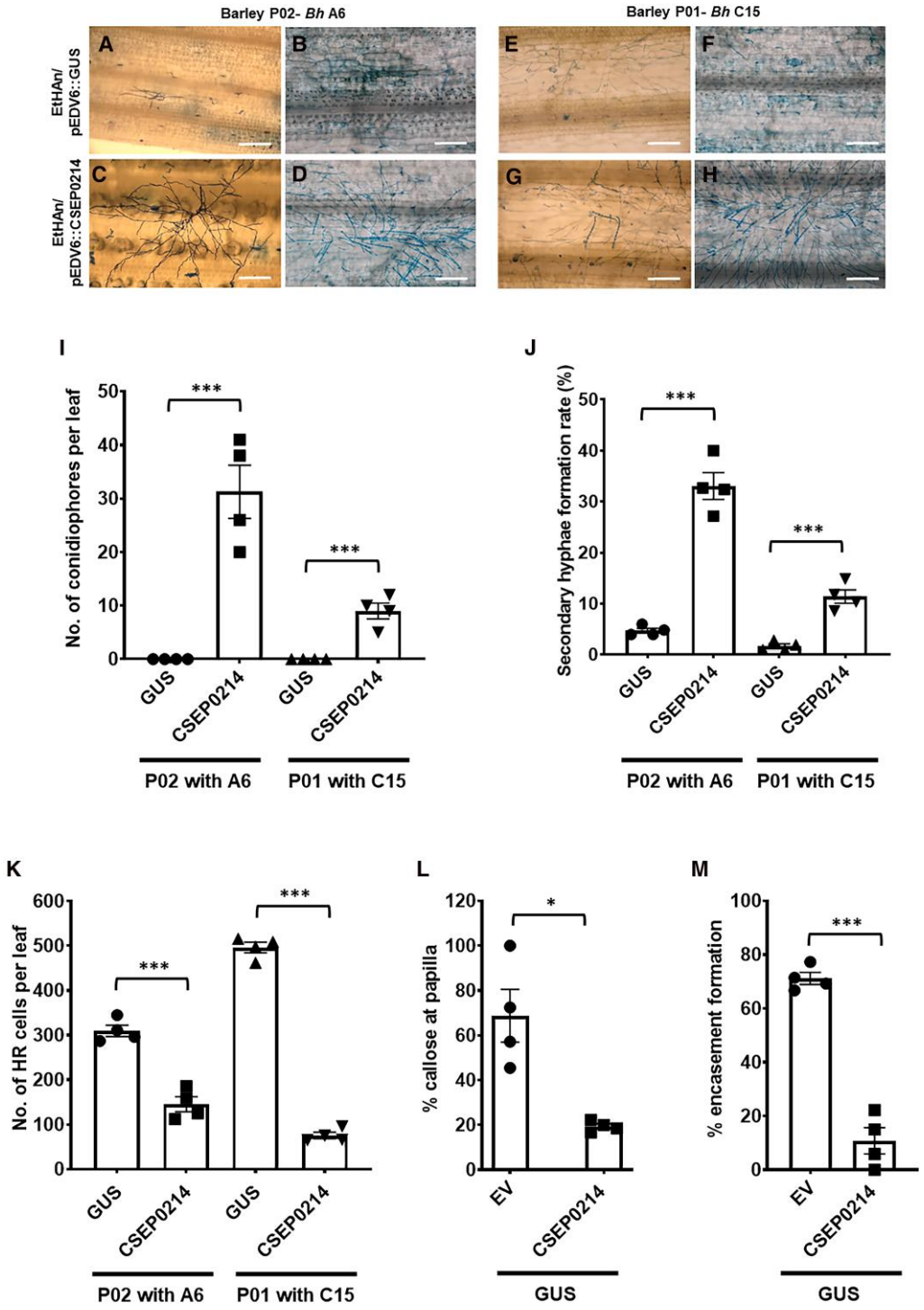


Figure 7. Expression of CSEP0214 inhibits CNL-mediated resistance, as well as papilla and encasement formation in response to *B. hordei*. **A-K)** *Mla3* (in P02) and *Mla1* (in P01)-mediated resistance to *Bh* in barley is broken by expression of CSEP0214. The EtHAn strain of *P. fluorescence* was used to introduce either β-GUS, as a control, or CSEP0214 into leaves of barley lines P02 or P01. The leaves were subsequently inoculated with the avirulent *Bh* isolates, A6 and C15, respectively. Samples were collected at 4 dpi and stained with either Coomassie blue (**A, C, E, G**) to visualize the fungal hyphae, or with trypan blue (**B, D, F, H**) to stain for cell death. Scale bars in (**A**-**H**), 200 µm. **I**, **J)** Pathogenic success of the fungus was quantified as the number of conidiophores per leaf of equal size (four leaves inspected per combination) (**I**) and the percentage of germinated spores forming hyphae (four leaves with a total of at least 100 spores analyzed per combination) (**J**). **K)** Cell death was measured as the number of cells showing a HR per leaf of equal size (four leaves with a total of at least 1,800 cells scored per combination), after staining with trypan blue four days post inoculation. **L)** Effect of CSEP0214 expression on callose deposition at papillae. Leaf epidermal cells of 7-day-old barley (cv. Golden Promise) plants were transformed by particle bombardment with a construct expressing GUS along with either EV (pUbi::GW) or expression of CSEP0214 (pUbi::CSEP0214). After one day, the leaves were inoculated with *Bh* (isolate C15). The percentage of GUS-positive cells with callose in the papilla in barley leaf epidermal cells was scored at 24 h post inoculation (hpi), by GUS staining, followed by aniline blue staining and observation with UV-epifluorescence microscopy (4 leaves with a total of at least 200 cells scored per combination). **M)** Effect of CSEP0214 expression on encasement of *Bh* (isolate C15) haustoria. Leaf epidermal cells of 7-day-old barley (cv. Golden Promise) plants were transformed as described in "L," treated with tetraconazole (100 µM) and inoculated with *Bh* (isolate C15) two hours later. After four days, the percentage of GUS-positive cells with callose-encased haustoria was scored, by observation with UV-fluorescence microscopy after aniline blue staining (four leaves with a total of at least 200 cells scored per combination). **I-M)** Error bars, SE. *, $P < 0.05$; ***, $P < 0.001$ assessed by Student's *t*-tests.

Downloaded from https://academic.oup.com/plphys/article/197/4/kiaf067/8026087 by Bibliothek der RWTH Aachen user on 09 February 2026

on selective medium indicating interaction between VPS18 and VPS16 (Fig. 8A). However, when CSEP0214 was coexpressed from pAG426-GPD-CSEP0214 along with VPS18 and VPS16, yeast growth was reduced, indicating a diminished interaction between VPS18 and VPS16 (Fig. 8A).

To validate this interference in planta, we coexpressed either RFP or RFP-VPS18 with Flag-VPS16 in *N. benthamiana* leaves, in the presence or absence of HA-tagged CSEP0214 (Fig. 8B). We used RFP trap beads to copurify the interacting partners from the cell lysate. We detected Flag-VPS16 in the IP blot with RFP-VPS18, but only when HA-CSEP0214 was absent (Fig. 8B). These Y2H and co-IP experiments indicate that CSEP0214 blocks the interaction between VPS18 and VPS16.

Discussion

In this study, we identified the CORVET and HOPS complex component VPS18 as a cellular target of the *Bh* core effector protein CSEP0214 (BLGH_02334). The genomes of powdery mildew fungi encode predicted effector arsenals that range from fewer than 100 putative effector genes in *P. polyspora* (Frantzeskakis et al. 2019) to more than 600 in the cereal-infecting pathogens of the genus *Blumeria* (Frantzeskakis et al. 2018; Müller et al. 2018), reviewed in (Barsoum et al. 2019). Here, we explored conservation of effector genes across the entire powdery mildew fungal lineage and identified seven genes that encode highly conserved effector proteins present in at least 15 out of the 16 powdery mildew fungal species analyzed (Fig. 1 and Supplementary Table S2). These effectors form the powdery mildew-specific core effectome expected to fulfill essential functions during host colonization and thus contribute to pathogenic success. As a result of this investigation, we also provide the scientific community with an in-depth analysis of the secretome of *Bh*, which updates and extends the results of a former study (Supplementary Table S1; Pedersen et al. 2012).

In view of the highly similar lifestyle and mode of pathogenicity of powdery mildew fungi and given the comparatively high number of effector genes in these species, the limited size of the identified core effectome, specific for this pathogen clade, is surprising. We cannot exclude that we underestimate the extent of the powdery mildew-specific core effectome due to the in part limited quality of the currently available powdery mildew genome assemblies. Nonetheless, it was already suggested that pathogenicity of powdery mildew fungi rests on a narrow core effectome that is augmented by a variable number of species/lineage-specific effectors required for the colonization of the various host plants (Liang et al. 2018).

We selected CSEP0214 (BLGH_02334), one of the seven powdery mildew core effectors, for detailed functional analysis. This effector was previously recognized as conserved between *B. graminis*, the Arabidopsis powdery mildew pathogen, *Golovinomyces orontii* and the pea powdery mildew *Erysiphe pisi* (Schmidt et al. 2014). Using an Y2H screen against a barley prey cDNA library, we identified VPS18 as a host protein that interacts with this effector. The CSEP0214-VPS18 interaction was seen in two different yeast systems, in biochemical co-IP experiments and in in planta luciferase complementation imaging assays (Fig. 3A to D; Supplementary Fig. S1), and we provide evidence that it is mediated by a number of molecular contacts along the two proteins (Fig. 4; Supplementary Fig. S7). The interaction is further supported by an SDS- and heat-resistant high-molecular-mass band detected with CSEP0214-specific antibodies in protein extract from infected barley leaves (Fig. 3E). The molecular mass of this band is consistent with the estimated mass of a VPS18-CSEP0214 complex, and the difficulty separating it is likely due to intricate molecular interactions, for instance involving the C-terminal RING domain of VPS18 and part of the CFEM domain of CSEP0214. Interestingly, some CFEM domain-containing effectors are critical for fungal virulence (Zhu et al. 2017; Bai et al. 2022; Wang et al. 2022; Zuo et al. 2022; Shang et al. 2024). In the grass pathogen *Fusarium graminearum*, for example, multiple CFEM effectors are essential for full virulence on maize as they negatively regulate the activity of a host cell wall-associated kinase (Zuo et al. 2022).

In plant–microbe interactions, membrane trafficking is a key process that is heavily targeted by effectors (Inada and Ueda 2014; Bhandari and Brandizzi 2024). It is required for the internalization of cell surface receptors (Beck et al. 2012), the secretion of antimicrobial cargo (Kim et al. 2014; Baena et al. 2022) and cell wall components (Sinclair et al. 2018), and possibly the accommodation of infection structures of certain pathogens (Berkey et al. 2017; Abubakar et al. 2023). VPS18 is a highly conserved core component of the CORVET and HOPS complexes that regulate endocytic membrane trafficking toward the plant vacuole, and the protein interacts with other HOPS and CORVET components, e.g. VPS16, VPS41, and VPS33, via its RING domain (Brillada et al. 2018; Takemoto et al. 2018; Hou et al. 2021). While oomycete pathogens employ effectors to redirect this endomembrane traffic toward their haustoria to generate the extrahaustorial membrane and bring resources to sustain them (Bozkurt et al. 2015; Gu et al. 2017; Petre et al. 2021; Jeon and Segonzac 2023; Yuen et al. 2023), we observe that the barley-powdery mildew fungus inhibits this pathway. The high expression level of CSEP0214 in the first 6 h after inoculation suggests that this inhibition is essential for the early phase of infection. The high amino acid conservation of this effector between powdery mildew fungi, which aligns with the highly conserved target, VPS18, further suggests that this inhibition is essential across powdery mildew fungal species. Our study of the truncations of CSEP0214 and VPS18 also indicate that this interaction is extremely strong, and spans the entire CSEP0214 protein (Fig. 4D; Supplementary Fig. S7). Thus, the identification of the CSEP0214-VPS18 interaction extends the growing list of plant endomembrane trafficking components that are targeted by powdery mildew effectors. For example, the *Bh* effector candidate BEC4 binds a barley ADP ribosylation factor-GTPase activating protein (ARF-GAP), thereby possibly affecting defense-associated vesicle trafficking in the host (Schmidt et al. 2014). Additionally, the *Bh* effector CSEP0162 associates with barley MON1, a component that is important for fusion of MVBs to their target membranes (Liao et al. 2023).

Here, we investigated membrane trafficking to the vacuole in relation to the effect of CSEP0214 on VPS18. Overall, we found that both expression of CSEP0214 and silencing of *VPS18* and other CORVET and HOPS components in barley cells impeded trafficking of the vacuolar marker protein, (SP)-RFP-AFVY (Fig. 5), the Golgi marker protein, ST-YFP (Supplementary Fig. S12A), the secreted protein, (SP)-mCherry (Supplementary Fig. S12B), and the immunity-associated PM syntaxin, ROR2 (Fig. 6). Instead, these marker proteins were partially retained in the ER, which strongly suggests that CSEP0214 indeed hampers VPS18 activity.

An open question is how inhibition of this late step in the endomembrane trafficking pathway causes the marker proteins to accumulate in the ER. We propose this is due to congestion of the system, resulting in failure of efficient trafficking of cargo receptors, glycosyltransferases, proteases, chaperones, and other proteins needed for the flow through the endomembrane trafficking pathway. Specific support for this idea is that CSEP0214 inhibits ST-YFP from taking the first step from the ER to its destination

Downloaded from https://academic.oup.com/plphys/article/197/4/kiaf067/8026087 by Bibliothek der RWTH Aachen user on 09 February 2026

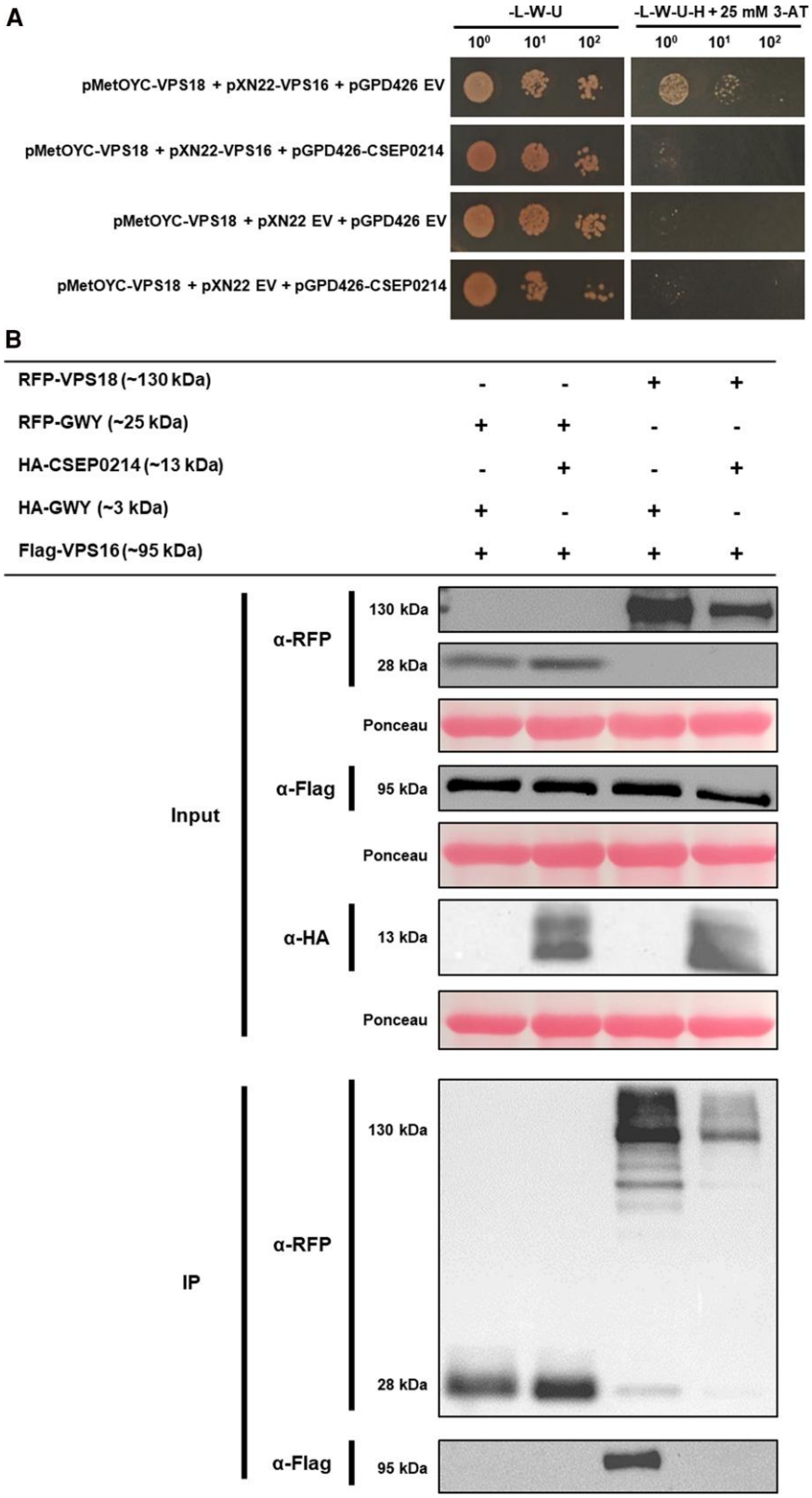


Figure 8. Expression of CSEP0214 inhibits interaction of VPS18 with VPS16. **A)** Three-way split-ubiquitin Y2H of FL barley VPS18 expressed from pMetOYC (VPS18-Cub-PLV) and FL barley VPS16 expressed from pXN22 (VPS16-NubG), in the presence or absence of pAG426-GPD-GW EV, or pAG426-GPD-CSEP0214 in the yeast strain THY.AP4. pMetOYC-VPS18 + EV pXN22 + EV pAG426-GPD-GW, and pMetOYC-VPS18 + EV pXN22 + pAG426-GPD-CSEP0214 served as negative controls. Aliquots of yeast liquid cultures were dropped in various dilutions on either SC-L-W-U medium (growth control) or SC-L-W-U-H + 25 mM 3-AT medium (interaction-selective). Images were taken after two days of growth. The experiment was performed twice with a similar outcome. **B)** Fusion proteins mRFP-VPS18, HA-CSEP0214 and Flag-VPS16 or the mRFP and HA tags alone, were coexpressed in different combinations via *A. tumefaciens*-mediated transient gene expression in leaves of *N. benthamiana* plants. Proteins were extracted for co-IP. Protein samples of the IP and the total protein extract (input) were used for SDS-PAGE and immunoblot analysis. The membranes were probed with α-RFP, α-Flag, and α-HA antibodies, respectively. On the left, molecular masses of marker proteins are given. Ponceau staining was used to demonstrate equal amount of total proteins on the blots. The experiment was performed three times with a similar outcome.

Downloaded from https://academic.oup.com/plphys/article/197/4/kiaf067/8026087 by Bibliothek der RWTH Aachen user on 09 February 2026

in the Golgi apparatus despite the fact that VPS18 acts late in the pathway. A similar scenario appears to occur in protoplasts of the Arabidopsis *mon1* mutant, also arrested in a later step in this pathway. In that system, the 2 vacuolar proteins RD21-YFP and Aleu-GFP accumulate in enlarged MVBs and seemingly also in the ER (Cui et al. 2017).

The orthologous barley ROR2 and Arabidopsis PEN1 syntaxins are required for penetration resistance and for timely papilla formation at the site of powdery mildew fungal attack (Collins et al. 2003; Assaad et al. 2004; Böhlenius et al. 2010). They also recycle from the PM to accumulate in papillae, where they label EVs (Bhat et al. 2005; Meyer et al. 2009; Böhlenius et al. 2010; Nielsen et al. 2012, 2017). Interestingly, this recycling is dependent on the flippase ALA3 that also mediates recycling of PEN3, an ABC transporter likewise required for penetration resistance (Underwood et al. 2017). Notwithstanding this, we noted that penetration resistance is not impeded by the overexpression of CSEP0214, VPS18, and the VPS18 RING domain (Supplementary Fig. S13), which affect the later steps in the endomembrane trafficking pathway. This outcome is consistent with earlier findings (Nielsen et al. 2017; Liao et al. 2023). Thus, ESCRT-dependent MVB formation may not be directly involved in the biosynthesis of papillae. Nevertheless, interference with VPS18 and VPS41 as well as expression of CSEP0214 hampered the accumulation of the ROR2 marker at the fungal attack sites (Fig. 6). While it may be straightforward to envisage how de novo synthesized proteins become arrested in the ER due to congestion when a late step in the endomembrane trafficking pathway is interfered with, it is less obvious how ROR2 recycling is affected. Notably, cross-regulation exists between ESCRT-independent and ESCRT-dependent pathways in mammalian cells (Wei et al. 2021), and similar mechanisms may exist in plants affecting the ROR2 recycling, when the ESCRT-dependent endomembrane pathway is clogged. We cannot exclude that CSEP0214 can have additional targets, explaining the observed effect on ROR2 recycling.

Delivery of CSEP0214 affected encasement formation, *Mla1* and *Mla3*-mediated resistance, and HR (Fig. 7). This is consistent with VPS18 interference and endomembrane pathway hampering, as encasement formation is dependent on the Rab5 GEF, VPS9a, as well as MON1 in Arabidopsis and barley (Nielsen et al. 2017; Liao et al. 2023). Also other CNL-mediated resistances require a functional endomembrane pathway. For example, HR activated by Arabidopsis RPM1 and RPS2 is dependent on the late endosome ESCRT components, AMSH3 and VPS4, in Arabidopsis and *N. benthamiana* (Schultz-Larsen et al. 2018), while barley-powdery mildew resistance mediated by the CNL *Mla3* requires MON1, the target of CSEP0162 (Liao et al. 2023).

It is unclear how the endomembrane pathway contributes to CNL-induced HR, as CNLs oligomerize and form Ca^{2+} channels located in the PM and possibly elsewhere (Bi et al. 2021). However, two separate adaptor protein complexes, AP-2 and AP-4, involved in clathrin-coated vesicle formation, are required for RPM1 and RPS2-mediated resistance, while AP-4 in addition is required for tonoplast-PM fusion (Hatsugai et al. 2016, 2018). We are looking forward to learn whether these adaptor protein functions link with the endomembrane pathway.

It is puzzling that EtHAn-introduced CSEP0214 can suppress resistance by at least two *Mla* variants (Fig. 7), and thus potentially target CNL-mediated resistance in general. Yet, even though *Bh* secretes these effectors, *Mla* resistance in barley is still functional. The existence of effectors with general NLR-mediated immunity inhibitory functions, referred to as "silver bullet" effectors, was previously questioned (Thordal-Christensen 2020). However, this view may have to be revised. In fact, EDS1, which has a general and shared function in immunity mediated by Toll-interleukin-1 receptor domain-containing NLRs (TNLs), has been described as an effector target (Bhattacharjee et al. 2011; Heidrich et al. 2011; Wang et al. 2014; Li et al. 2020). Thus, it appears that the barley-powdery mildew fungus and other pathogens indeed secrete effectors that impede NLR functions in general. The puzzle is how NLRs can be fully effective despite the existence of such broadly acting effectors. Possible explanations could be the lower expression levels of these effectors in the natural situation and/or their timing of expression.

Additionally, we shed light on the mechanism of action of CSEP0214, and provide evidence that CSEP0214 blocks the function of VPS18 by interfering with its interaction with VPS16 (Fig. 8). VPS18 and VPS16 are shared components of the HOPS and CORVET tethering complexes. Additionally, VPS16 and VPS33 together form the SNARE-binding module of these complexes (Graham et al. 2013; Baker and Hughson 2016). Our observed CSEP0214-mediated interference of the VPS18/VPS16 binding would result in a loss of the SNARE-binding module of these tethering complexes. Thus, we suggest that expression of the effector CSEP0214 blocks the vacuolar pathway by inhibition of the activity of the CORVET and HOPS. This block is likely achieved by direct attachment of CSEP0214 to the RING domain of VPS18 (found in our Y2H cDNA screen), which is also the VPS16-binding surface in VPS18 (Shvarev et al. 2022). In conclusion, we have discovered that powdery mildew fungi share core effectors and one of them, CSEP0214, targets barley VPS18. We provide evidence that CSEP0214 inhibits the interaction of VPS18 and VPS16 of the endomembrane trafficking machinery transmitting material to the vacuole and for the secretion of EVs. Since this pathway is central for encasement formation and CNL-mediated immunity, we hypothesize that CSEP0214 makes a significant contribution to the virulence of *Bh*.

Materials and methods

In silico analyses

The basis for the *B. hordei* (*Bh*) effector in silico analyses was the predicted secretome as defined by the 2018 annotation of the *Bh* genome (Frantzeskakis et al. 2018). Details of the bioinformatics analysis performed can be found in Supplementary File 1.

Plant material and growth conditions

Barley (*H. vulgare*) plants were grown in a climate chamber (16 h light (150 μE m^{-2} s^{-1})/8 h dark, at 20 °C, 60% relative humidity). Susceptible barley cultivar (cv.) Golden Promise seedlings and the *Bh* isolate C15 were used for transient expression analysis, subcellular localization, callose staining, and RNAi experiments. Susceptible barley cv. Lottie was used in combination with the *Bh* isolate K1 for experiments to score host cell entry rates upon transient gene expression. Near-isogenic lines P01 and P02 of barley cv. Pallas (Kølster et al. 1986) and the *Bh* isolates A6 and C15 were used to study resistance mediated by the *Mla1* and *Mla3* genes, respectively. *N. benthamiana* plants were used for co-IP experiments as well as luciferase complementation imaging assays and were grown in a controlled growth chamber (16 h light (150 μE m^{-2} s^{-1}) at 23 °C/8 h dark at 20 °C, 60% relative humidity).

Barley Y2H cDNA prey library

The used cDNA prey library was generated from leaf epidermal peels of two barley cultivars, inoculated with two different *Bh* isolates and sampled at six different time points prior to/after

Downloaded from https://academic.oup.com/plphys/article/197/4/kiaf067/8026087 by Bibliothek der RWTH Aachen user on 09 February 2026

inoculation: Primary leaves of 6-to-7-day-old barley cv. Golden Promise seedlings were inoculated with *Bh* isolate DH14, while barley cv. Margret seedlings were inoculated with *Bh* isolate K1. Epidermal peels were collected at 0, 6, 12, 24, 48, and 96 hpi. Total RNA was extracted with the Qiagen RNeasy Plant Mini Kit (Qiagen, Hilden, Germany) and sent to ThermoFisher Scientific (Waltham, Massachusetts, USA) for cDNA library construction in pDEST22 (Y2H prey vector) based on oligo-dT-primed cDNA synthesis.

Cloning

Barley and *Bh* cDNA coding sequences were amplified from RNA from infected barley plants, and cloned via Gateway BP reaction into pDONR201 or pDONR207 or by TOPO cloning reaction into pENTR/D-TOPO, according to the manufacturer's protocol. Clones confirmed by sequencing were used for Gateway LR reaction into different destination vectors (see Supplementary Table S4).

GAL4-based Y2H and split-ubiquitin Y2H experiments

Yeast cells were transformed following the standard LiAc-mediated protocol (Gietz and Woods 2002). The heat shock at 42 °C was performed for 10 min for the PJ69-4A strain (James et al. 1996) (GAL4-based Y2H assays), and for 1 h for the THY.AP4 strain (Grefen et al. 2009) (split-ubiquitin Y2H experiments). Bait protein expression was verified via immunoblot with an α-GAL4 DBD antibody (Santa Cruz Biotechnology) or LexA antibody (gift by Karin Römisch), respectively. Yeast plasmid isolation was performed as described (Robzyk and Kassir 1992). Yeast protein extraction was performed according to a protocol from the Dohlman Lab (https://www.med.unc.edu/pharm/dohlmanlab/resources/lab-methods/tca/; Cox et al. 1997). The supernatant was used for the assessment of protein concentration by Bradford assay and immunoblot analysis.

Coimmunoprecipitation

Agrobacterium tumefaciens strain GV3101 (pMP90RK) was used for transient gene expression in leaves of *N. benthamiana*, which were harvested at two days after *A. tumefaciens* infiltration for protein extraction in 50 mM Tris-HCl pH 8.0, 1 mM EDTA, 1 mM dithiothreitol, supplemented with Complete Mini protease inhibitor cocktail (Roche, Mannheim, Germany). Protein concentration was determined by the Bradford assay (Bradford 1976), and 500 µg total protein was used for immunoprecipitation (IP) using α-RFP-Trap agarose or magnetic-agarose beads (ChromoTek GmbH, Planegg, Germany). Samples of the soluble fraction (Input) and the bead-associated proteins (IP) were used for SDS-PAGE and immunoblot analysis using standard procedures. Details of antibodies used can be found in Supplementary Table S4.

Luciferase complementation imaging

Luciferase complementation imaging experiments were essentially conducted as described before (Spiller et al. 2023; von Bongartz et al. 2023; Huebbers et al. 2024). Briefly, *VPS18*, *CSEP0214*, *CSEP0051*, and *CSEP0061* coding sequences (the latter three lacking their SP) were shuttled by Gateway recombination into destination vectors suitable for luciferase complementation imaging assays (pAMPAT-CLuc-GWY, pAMPAT-NLuc-GWY, pAMPAT-GWY-CLuc, and pAMPAT-GWY-NLuc; Gruner et al. 2021). Agrobacteria harboring appropriate combinations were coinfiltrated into the abaxial side of *N. benthamiana* leaves, these incubated for three days, and 1 mM D-luciferin (Sigma-Aldrich, Darmstadt, Germany) sprayed on their surface. After incubation for 10 min in the dark, luminescence was detected with a ChemiDoc XRS+ imaging system (Bio-Rad, Feldkirchen, Germany) and evaluated using the Image Lab software (Bio-Rad, version 6.1). Expression of luciferase complementation imaging constructs in *N. benthamiana* was validated by immunoblot analysis using an α-luciferase rabbit polyclonal primary antibody (Merck, Darmstadt, Germany; diluted 1:1000).

Immunoblot detection of CSEP0214

An antiserum was raised in rabbit against two CSEP0214-derived peptides (HTEGGKGGKGGKGDDDGDDD and IDAGCKSAADFACT CEHDTNKA), individually coupled to KLH carrier protein and designed to cover the predicted disordered region and the CFEM domain, respectively, and the resulting blood serum affinity-purified against either the first or second peptide (Davids Biotechnologie GmbH, Regenburg, Germany). Total protein extract from non-infected and *Bh*-infected barley leaves sampled at five days post inoculation (dpi) were used for immunoblot analysis. For detection of purified recombinant CSEP0214 protein from *E. coli*, the Rosetta strain was transformed with pDEST15-RFP or pDEST17-CSEP0214 protein expression constructs, induced with 1 mM isopropyl-β-D-thiogalactopyranoside, and incubated at 16 °C overnight. Cell extract was obtained by sonication, which was further used for SDS-PAGE and immunoblot analysis.

Transient expression of gene constructs in barley

Transformation of gene constructs into leaf epidermal cells of the abaxial side of 7-day-old barley seedlings was conducted by particle bombardment as described before (Douchkov et al. 2005) using 1 µm gold particles via the Bio-Rad PDS-1000/He particle delivery system, mounted with a hepta-adapter, according to the manufacturer's instructions (Bio-Rad). Fluorescent signals emitted by mCherry, RFP (laser line with excitation of 587 nm and emission wavelengths 596—644 nm) or mYFP (laser line with excitation of 508 nm and emission wavelengths of 513—575 nm) were visualized using a Leica (Wetzlar, Germany) Stellaris 8 confocal laser scanning microscope. Laser intensities and gains were variable and adjusted for each image as expression levels vary from cell to cell in single cell analyses as done here. See Supplementary Table S4 for a list of the marker constructs used in this work.

Study of immune responses

Papilla formation, penetration resistance, and encasement formation were studied after transient transformation of barley leaf epidermal cells with the respective constructs in combination with a construct for β-GUS expression (Douchkov et al. 2005), followed by inoculation with *Bh*, and aniline blue staining, which was subsequently assessed by UV epifluorescence microscopy. Papilla formation was studied at 1 dpi whereas penetration resistance was studied at 2 dpi. Encasement formation was studied 4 dpi after bombardment and tetraconazole treatment (100 µg/ml tetraconazole in 20% acetone with 0.04% Tween-20; Maffi et al. 1995). To study HR and fungal development, the EtHAn strain of *P. fluorescence* (Thomas et al. 2009) was used, followed by inoculation with avirulent *Bh* isolates C15 and A6, respectively. Cells undergoing HR were stained with trypan blue as described before (Koch and Slusarenko 1990) and fungal structures were visualized by Coomassie staining as above. Scoring was performed by light microscopy at 4 dpi.

Downloaded from https://academic.oup.com/plphys/article/197/4/kiaf067/8026087 by Bibliothek der RWTH Aachen user on 09 February 2026

Accession numbers

Sequence data from this article can be found in the GenBank/EMBL data libraries under accession numbers _ AEQ16460.1 (*B. hordei* CSEP0214/BLGH_02334), XP_044984692 (*H. vulgare VPS18*), XP_044968511 (*H. vulgare VPS41*), and AY246907.1 (*H. vulgare Ror2*).

Acknowledgments

We acknowledge the support of many helping hands in the Panstruga and Spanu labs (amongst others Lamprinos Frantzeskakis, Hannah Kuhn, Hongpo Wu, Linhan Li, and Helen Pennington) regarding the isolation of epidermal peels for cDNA construction. We thank our late and good friend, Dr. Patrick Schweizer (Leibniz Institute of Plant Genetics and Crop Plant Research, Gatersleben, Germany) for providing the RNAi vector. We appreciate the cloning of the pAMpat-SP-mCherry construct by Mark Kwaaitaal and Meike Lauts. We thank the Centre for Advanced Bioimaging (CAB) at the University of Copenhagen for use of their facilities. Furthermore, we thank Prof. Chris Hawes for making the ST–YFP construct available to us. We thank Prof. Andreas Nebenführ for the SP–mCherry–HDEL construct. We are grateful to Prof. Jeff Chang for providing the EtHAn bacterial strain and Prof. Jonathan Jones for allowing us to use the pEDV6 vector. We thank Karin Römisch (Saarland University, Germany) for sharing the LexA antibody with us.

Author contributions

B.S. performed the in silico CSEP analysis and conducted Y2H and co-IP assays. S.D. performed all cell biological (co-)localization and immune response studies and performed Y2H and co-IP assays. S.C.J.L., M.F., and A.R. performed luciferase complementation assays. H.T.C. and R.P. conceived the study and supervised the project. P.D.S. and R.P. designed the Y2H prey library and coordinated their synthesis. B.S. (with the help of others) collected material for the Y2H library. B.S. and S.D. drafted the manuscript. P.D.S., H.T.C., and R.P. edited the manuscript.

Supplementary data

The following materials are available in the online version of this article.

Supplementary Figure S1. Interaction of CSEP0214 with VPS18.

Supplementary Figure S2. Specificity of the CSEP0214 and VPS18 interaction.

Supplementary Figure S3. Testing the α-CSEP0214 antibody with His-CSEP0214 heterologously expressed in *E. coli*.

Supplementary Figure S4. Self-interaction of CSEP0214.

Supplementary Figure S5. CSEP0214 and VPS18 form a stable, heat-resistant protein complex.

Supplementary Figure S6. Y2H assay of the VPS18 RING domain with truncated variants of CSEP0214.

Supplementary Figure S7. Split-ubiquitin Y2H assay of FL VPS18 with truncated variants of CSEP0214.

Supplementary Figure S8. Predicted three-dimensional structure of barley VPS18.

Supplementary Figure S9. The expression of VPS18, VPS41 or their RING domains in barley leaf epidermal cells blocks the transport of a vacuolar marker protein.

Supplementary Figure S10. Transient knockdown of *VPS8* in barley leaf epidermal cells perturbs the subcellular localization of vacuolar and papilla markers.

Supplementary Figure S11. Expression of VPS18, VPS41 or their RING domains in barley leaf epidermal cells blocks the transport and accumulation of the papilla marker protein ROR2.

Supplementary Figure S12. CSEP0214 expression in barley leaf epidermal cells perturbs the subcellular localization of endomembrane trafficking pathway markers.

Supplementary Figure 13. Expression of CSEP0214, VPS18 or VPS18 RING does not affect the fungal host cell penetration rate.

Supplementary Table S1. In silico analysis of the *Bh* secretome.

Supplementary Table S2. The powdery mildew effectome.

Supplementary Table S3. Hits of the Y2H cDNA library screen using CSEP0214 as a bait.

Supplementary Table S4. List of primers, clones, cellular markers and antibodies used.

Supplementary File 1. Details of the in silico analysis of *B. hordei* secreted proteins.

Funding

This work was funded by the Novo Nordisk Fonden grant NNF19OC0056457 (PlantsGoImmune) to R.P. and H.T.C., Villum Fonden grants 00028131 and 00050260 to H.T.C., and Horizon Europe Marie Skłodowska-Curie Actions project 101104193 to S.D. The barley cDNA library was generated within the European Research Area Network for Coordinating Action in Plant Sciences (ERA-CAPS)-funded project DURESTrit (Deutsche Forschungsgemeinschaft (DFG) grant PA 861/13-1, project number 243085332 to RP and Biotechnology and Biological Sciences Research Council (BBSRC) grant BB/M000710/1 to PDS)).

Conflict of interest statement. None declared.

Data availability

The data underlying this article are available in the article and in its online supplementary material.

References

Abubakar YS, Sadiq IZ, Aarti A, Wang Z, Zheng W. Interplay of transport vesicles during plant-fungal pathogen interaction. *Stress Biol.* 2023:3(1):35. https://doi.org/10.1007/s44154-023-00114-0

Aguilar GB, Pedersen C, Thordal-Christensen H. Identification of eight effector candidate genes involved in early aggressiveness of the barley powdery mildew fungus. *Plant Pathol.* 2016:65(6):953–958. https://doi.org/10.1111/ppa.12476

Ahmed AA, Pedersen C, Schultz-Larsen T, Kwaaitaal M, Jørgensen HJL, Thordal-Christensen H. The barley powdery mildew candidate secreted effector protein CSEP0105 inhibits the chaperone activity of a small heat shock protein. *Plant Physiol.* 2015:168(1):321–333. https://doi.org/10.1104/pp.15.00278

Ahmed AA, Pedersen C, Thordal-Christensen H. The barley powdery mildew effector candidates CSEP0081 and CSEP0254 promote fungal infection success. *PLoS One*. 2016:11(6):e0157586. https://doi.org/10.1371/journal.pone.0157586

Alberti S, Gitler AD, Lindquist S. A suite of gateway cloning vectors for high-throughput genetic analysis in *Saccharomyces cerevisiae*. *Yeast*. 2007:24(10):913–919. https://doi.org/10.1002/yea.1502

Assaad FF, Qiu J-L, Youngs H, Ehrhardt D, Zimmerli L, Kalde M, Wanner G, Peck SC, Edwards H, Ramonell K, *et al.* The PEN1 syntaxin defines a novel cellular compartment upon fungal attack

Downloaded from https://academic.oup.com/plphys/article/197/4/kiaf067/8026087 by Bibliothek der RWTH Aachen user on 09 February 2026

and is required for the timely assembly of papillae. *Mol Biol Cell*. 2004:15(11):5118–5129. https://doi.org/10.1091/mbc.e04-02-0140

Baena G, Xia L, Waghmare S, Karnik R. SNARE SYP132 mediates divergent traffic of plasma membrane H^+-ATPase AHA1 and antimicrobial PR1 during bacterial pathogenesis. *Plant Physiol*. 2022:189(3):1639–1661. https://doi.org/10.1093/plphys/kiac149

Bai X, Peng H, Goher F, Islam MA, Xu S, Guo J, Kang Z, Guo J. A candidate effector protein PstCFEM1 contributes to virulence of stripe rust fungus and impairs wheat immunity. *Stress Biol*. 2022:2(1):21. https://doi.org/10.1007/s44154-022-00042-5

Baker RW, Hughson FM. Chaperoning SNARE assembly and disassembly. *Nat Rev Mol Cell Biol*. 2016:17(8):465–479. https://doi.org/10.1038/nrm.2016.65

Balderhaar HJ, Ungermann C. CORVET and HOPS tethering complexes—coordinators of endosome and lysosome fusion. *J Cell Sci*. 2013:126(6):1307–1316. https://doi.org/10.1242/jcs.107805

Barsoum M, Sabelleck B, Spanu PD, Panstruga R. Rumble in the effector jungle: candidate effector proteins in interactions of plants with powdery mildew and rust fung. *Crit Rev Plant Sci*. 2019:38(4):255–279. https://doi.org/10.1080/07352689.2019.1653514

Beck M, Heard W, Mbengue M, Robatzek S. The INs and OUTs of pattern recognition receptors at the cell surface. *Curr Opin Plant Biol*. 2012:15(4):367–374. https://doi.org/10.1016/j.pbi.2012.05.004

Berkey R, Zhang Y, Ma X, King H, Zhang Q, Wang W, Xiao S. Homologues of the RPW8 resistance protein are localized to the extrahaustorial membrane that is likely synthesized de novo. *Plant Physiol*. 2017:173(1):600–613. https://doi.org/10.1104/pp.16.01539

Bhandari DD, Brandizzi F. Logistics of defense: the contribution of endomembranes to plant innate immunity. *J Cell Biol*. 2024:223(6):e202307066. https://doi.org/10.1083/jcb.202307066

Bhat RA, Miklis M, Schmelzer E, Schulze-Lefert P, Panstruga R. Recruitment and interaction dynamics of plant penetration resistance components in a plasma membrane microdomain. *Proc Natl Acad Sci U S A*. 2005:102(8):3135–3140. https://doi.org/10.1073/pnas.0500012102

Bhattacharjee S, Halane MK, Kim SH, Gassmann W. Pathogen effectors target Arabidopsis EDS1 and alter its interactions with immune regulators. *Science*. 2011:334(6061):1405–1408. https://doi.org/10.1126/science.1211592

Bi G, Su M, Li N, Liang Y, Dang S, Xu J, Hu M, Wang J, Zou M, Deng Y, *et al*. The ZAR1 resistosome is a calcium-permeable channel triggering plant immune signaling. *Cell*. 2021:184(13):3528–3541.e12. https://doi.org/10.1016/j.cell.2021.05.003

Bindschedler LV, Panstruga R, Spanu PD. Mildew-omics: how global analyses aid the understanding of life and evolution of powdery mildews. *Front Plant Sci*. 2016:7:123. https://doi.org/10.3389/fpls.2016.00123

Blum M, Chang H-Y, Chuguransky S, Grego T, Kandasaamy S, Mitchell A, Nuka G, Paysan-Lafosse T, Qureshi M, Raj S, *et al*. The InterPro protein families and domains database: 20 years on. *Nucleic Acids Res*. 2021:49(D1):D344–D354. https://doi.org/10.1093/nar/gkaa977

Böhlenius H, Mørch SM, Godfrey D, Nielsen ME, Thordal-Christensen H. The multivesicular body-localized GTPase ARFA1b/1c is important for callose deposition and ROR2 syntaxin-dependent preinvasive basal defense in barley. *Plant Cell*. 2010:22(11):3831–3844. https://doi.org/10.1105/tpc.110.078063

Bozkurt TO, Belhaj K, Dagdas YF, Chaparro-Garcia A, Wu C-H, Cano LM, Kamoun S. Rerouting of plant late endocytic trafficking toward a pathogen interface. *Traffic*. 2015:16(2):204–226. https://doi.org/10.1111/tra.12245

Bradford MM. A rapid and sensitive method for the quantitation of microgram quantities of protein utilizing the principle of protein-dye binding. *Anal Biochem*. 1976:72(1–2):248–254. https://doi.org/10.1016/0003-2697(76)90527-3

Brandizzi F, Snapp EL, Roberts AG, Lippincott-Schwartz J, Hawes C. Membrane protein transport between the endoplasmic reticulum and the Golgi in tobacco leaves is energy dependent but cytoskeleton independent: evidence from selective photobleaching. *Plant Cell*. 2002:14(6):1293–1309. https://doi.org/10.1105/tpc.001586

Braun U, Cook RTA. *Taxonomic manual of the Erysiphales (powdery mildews)*. Vol 11. Utrecht, The Netherlands: CBS-KNAW Fungal Biodiversity Centre; 2012.

Brillada C, Zheng J, Krüger F, Rovira-Diaz E, Askani JC, Schumacher K, Rojas-Pierce M. Phosphoinositides control the localization of HOPS subunit VPS41, which together with VPS33 mediates vacuole fusion in plants. *Proc Natl Acad Sci U S A*. 2018:115(35):E8305–E8314. https://doi.org/10.1073/pnas.1807763115

Chen HM, Zou Y, Shang Y, Lin H, Wang Y, Cai R, Tang X, Zhou J-M. Firefly luciferase complementation imaging assay for protein-protein interactions in plants. *Plant Physiol*. 2008:146(2):368–376. https://doi.org/10.1104/pp.107.111740

Collins NC, Thordal-Christensen H, Lipka V, Bau S, Kombrink E, Qiu J-L, Hückelhoven R, Stein M, Freialdenhoven A, Somerville SC, *et al*. SNARE-protein-mediated disease resistance at the plant cell wall. *Nature*. 2003:425(6961):973–977. https://doi.org/10.1038/nature02076

Cox JS, Chapman RE, Walter P. The unfolded protein response coordinates the production of endoplasmic reticulum protein and endoplasmic reticulum membrane. *Mol Biol Cell*. 1997:8(9):1805–1814. https://doi.org/10.1091/mbc.8.9.1805

Cui Y, Zhao Q, Xie H-T, Wong WS, Wang X, Gao C, Ding Y, Tan Y, Ueda T, Zhang Y, *et al*. MONENSIN SENSITIVITY1 (MON1)/CALCIUM CAFFEINE ZINC SENSITIVITY1 (CCZ1)-mediated Rab7 activation regulates tapetal programmed cell death and pollen development. *Plant Physiol*. 2017:173(1):206–218. https://doi.org/10.1104/pp.16.00988

Douchkov D, Nowara D, Zierold U, Schweizer P. A high-throughput gene-silencing system for the functional assessment of defense-related genes in barley epidermal cells. *Mol Plant Microbe Interact*. 2005:18(8):755–761. https://doi.org/10.1094/MPMI-18-0755

Fabro G, Steinbrenner J, Coates M, Ishaque N, Baxter L, Studholme DJ, Körner E, Allen RL, Piquerez SJM, Rougon-Cardoso A, *et al*. Multiple candidate effectors from the oomycete pathogen *Hyaloperonospora arabidopsidis* suppress host plant immunity. *PLoS Pathog*. 2011:7(11):e1002348. https://doi.org/10.1371/journal.ppat.1002348

Frantzeskakis L, Kracher B, Kusch S, Yoshikawa-Maekawa M, Bauer S, Pedersen C, Spanu PD, Maekawa T, Schulze-Lefert P, Panstruga R. Signatures of host specialization and a recent transposable element burst in the dynamic one-speed genome of the fungal barley powdery mildew pathogen. *BMC Genomics*. 2018:19(1):381. https://doi.org/10.1186/s12864-018-4750-6

Frantzeskakis L, Németh MZ, Barsoum M, Kusch S, Kiss L, Takamatsu S, Panstruga R. The *Parauncinula polyspora* draft genome provides insights into patterns of gene erosion and genome expansion in powdery mildew fungi. *mBio*. 2019:10(5):e01692-19. https://doi.org/10.1128/mBio.01692-19

Gietz RD, Woods RA. Transformation of yeast by lithium acetate/single-stranded carrier DNA/polyethylene glycol method. In: Fink GR, Guthrie C, editors, *Guide to yeast genetics and molecular and cell biology*, Vol 350. Amsterdam: Academic Pr; 2002. p. 87–96.

Downloaded from https://academic.oup.com/plphys/article/197/4/kiaf067/8026087 by Bibliothek der RWTH Aachen user on 09 February 2026

Graham SC, Wartosch L, Gray SR, Scourfield EJ, Deane JE, Luzio JP, Owen DJ. Structural basis of Vps33A recruitment to the human HOPS complex by Vps16. *Proc Natl Acad Sci U S A*. 2013:110(33): 13345–13350. https://doi.org/10.1073/pnas.1307074110

Grefen C, Obrdlik P, Harter K. The determination of protein-protein interactions by the mating-based split-ubiquitin system (mbSUS). *Methods Mol Biol*. 2009:479:217–233. https://doi.org/10.1007/978-1-59745-289-2_14

Gruner K, Leissing F, Sinitski D, Thieron H, Axstmann C, Baumgarten K, Reinstädler A, Winkler P, Altmann M, Flatley A, *et al.* Chemokine-like MDL proteins modulate flowering time and innate immunity in plants. *J Biol Chem*. 2021:296:100611. https://doi.org/10.1016/j.jbc.2021.100611

Gu Y, Zavaliev R, Dong X. Membrane trafficking in plant immunity. *Mol Plant*. 2017:10(8):1026–1034. https://doi.org/10.1016/j.molp.2017.07.001

Hatsugai N, Hillmer R, Yamaoka S, Hara-Nishimura I, Katagiri F. The μ subunit of *Arabidopsis* adaptor protein-2 is involved in effector-triggered immunity mediated by membrane-localized resistance proteins. *Mol Plant Microbe Interact*. 2016:29(5):345–351. https://doi.org/10.1094/MPMI-10-15-0228-R

Hatsugai N, Nakatsuji A, Unten O, Ogasawara K, Kondo M, Nishimura M, Shimada T, Katagiri F, Hara-Nishimura I. Involvement of adapter protein complex 4 in hypersensitive cell death induced by avirulent bacteria. *Plant Physiol*. 2018:176(2): 1824–1834. https://doi.org/10.1104/pp.17.01610

Heidrich K, Wirthmueller L, Tasset C, Pouzet C, Deslandes L, Parker JE. *Arabidopsis* EDS1 connects pathogen effector recognition to cell compartment–specific immune responses. *Science*. 2011: 334(6061):1401–1404. https://doi.org/10.1126/science.1211641

Hou S, Shi J, Hao L, Wang Z, Liao Y, Gu H, Dong J, Dresselhaus T, Zhong S, Qu L-J. VPS18-regulated vesicle trafficking controls the secretion of pectin and its modifying enzyme during pollen tube growth in Arabidopsis. *Plant Cell*. 2021:33(9):3042–3056. https://doi.org/10.1093/plcell/koab164

Huebbers JW, Caldarescu GA, Kubátová Z, Sabol P, Levecque SCJ, Kuhn H, Kulich I, Reinstädler A, Büttgen K, Manga-Robles A, *et al.* Interplay of EXO70 and MLO proteins modulates trichome cell wall composition and susceptibility to powdery mildew. *Plant Cell*. 2024:36(4):1007–1035. https://doi.org/10.1093/plcell/koad319

Hunter PR, Craddock CP, Di Benedetto S, Roberts LM, Frigerio L. Fluorescent reporter proteins for the tonoplast and the vacuolar lumen identify a single vacuolar compartment in Arabidopsis cells. *Plant Physiol*. 2007:145(4):1371–1382. https://doi.org/10.1104/pp.107.103945

Inada N, Ueda T. Membrane trafficking pathways and their roles in plant-microbe interactions. *Plant Cell Physiol*. 2014:55(4):672–686. https://doi.org/10.1093/pcp/pcu046

Irons SL, Evans DE, Brandizzi F. The first 238 amino acids of the human lamin B receptor are targeted to the nuclear envelope in plants. *J Exp Bot*. 2003:54(384):943–950. https://doi.org/10.1093/jxb/erg102

James P, Halladay J, Craig EA. Genomic libraries and a host strain designed for highly efficient two-hybrid selection in yeast. *Genetics*. 1996:144(4):1425–1436. https://doi.org/10.1093/genetics/144.4.1425

Jeon H, Segonzac C. Manipulation of the host endomembrane system by bacterial effectors. *Mol Plant Microbe Interact*. 2023:36(4): 208–217. https://doi.org/10.1094/MPMI-09-22-0190-FI

Jones JDG, Dangl JL. The plant immune system. *Nature*. 2006: 444(7117):323–329. https://doi.org/10.1038/nature05286

Kao Y-T, Fleming WA, Ventura MJ, Bartel B. Genetic interactions between PEROXIN12 and other peroxisome-associated ubiquitination components. *Plant Physiol*. 2016:172(3):1643–1656. https://doi.org/10.1104/pp.16.01211

Kim H, O'Connell R, Maekawa-Yoshikawa M, Uemura T, Neumann U, Schulze-Lefert P. The powdery mildew resistance protein RPW8.2 is carried on VAMP721/722 vesicles to the extrahaustorial membrane of haustorial complexes. *Plant J*. 2014:79(5):835–847. https://doi.org/10.1111/tpj.12591

Koch E, Slusarenko A. Arabidopsis is susceptible to infection by a downy mildew fungus. *Plant Cell*. 1990:2(5):437–445. https://doi.org/10.1105/tpc.2.5.437

Kølster P, Munk L, Stølen O, Løhde J. Near-isogenic barley lines with genes for resistance to powdery mildew. *Crop Sci*. 1986:26(5): 903–907. https://doi.org/10.2135/cropsci1986.0011183X00260005 0014x

Kulkarni RD, Kelkar HS, Dean RA. An eight-cysteine-containing CFEM domain unique to a group of fungal membrane proteins. *Trends Biochem Sci*. 2003:28(3):118–121. https://doi.org/10.1016/S0968-0004(03)00025-2

Li Q, Wang J, Bai T, Zhang M, Jia Y, Shen D, Zhang M, Dou D. A *Phytophthora capsici* effector suppresses plant immunity via interaction with EDS1. *Mol. Plant Pathol*. 2020:21(4):502–511. https://doi.org/10.1111/mpp.12912

Li X, Jin C, Yuan H, Huang W, Liu F, Fan R, Xie J, Shen Q-H. The barley powdery mildew effectors CSEP0139 and CSEP0182 suppress cell death and promote *B. graminis* fungal virulence in plants. *Phytopathol Res*. 2021:3(1):7. https://doi.org/10.1186/s42483-021-00084-z

Li Z, Velásquez-Zapata V, Elmore JM, Li X, Xie W, Deb S, Tian X, Banerjee S, Jørgensen HJL, Pedersen C, *et al.* Powdery mildew effectors AVR_{A1} and BEC1016 target the ER J-domain protein HvERdj3B required for immunity in barley. *Mol Plant Pathol*. 2024:25(5):e13463. https://doi.org/10.1111/mpp.13463

Liang P, Liu S, Xu F, Jiang S, Yan J, He Q, Liu W, Lin C, Zheng F, Wang X, *et al.* Powdery mildews are characterized by contracted carbohydrate metabolism and diverse effectors to adapt to obligate biotrophic lifestyle. *Front Microbiol*. 2018:9:3160. https://doi.org/10.3389/fmicb.2018.03160

Liao W, Nielsen ME, Pedersen C, Xie W, Thordal-Christensen H. Barley endosomal MONENSIN SENSITIVITY1 is a target of the powdery mildew effector CSEP0162 and plays a role in plant immunity. *J Exp Bot*. 2023:74(1):118–129. https://doi.org/10.1093/jxb/erac403

Liu M, Braun U, Takamatsu S, Hambleton S, Shoukouhi P, Bisson KR, Hubbard K. Taxonomic revision of *Blumeria* based on multi-gene DNA sequences, host preferences and morphology. *Mycoscience*. 2021:62(3):143–165. https://doi.org/10.47371/mycosci.2020.12.003

Maffi D, Cozzi F, Violini G, Bassi M, Conti GG. Ultrastructural studies of the effects of tetraconazole on the barley-powdery mildew host pathogen complex. *Mycol Res*. 1995:99(7):799–805. https://doi.org/10.1016/S0953-7562(09)80729-6

Meyer D, Pajonk S, Micali C, O'Connell R, Schulze-Lefert P. Extracellular transport and integration of plant secretory proteins into pathogen-induced cell wall compartments. *Plant J*. 2009:57(6):986–999. https://doi.org/10.1111/j.1365-313X.2008.03743.x

Müller MC, Praz CR, Sotiropoulos AG, Menardo F, Kunz L, Schudel S, Oberhänsli S, Poretti M, Wehrli A, Bourras S, *et al.* A chromosome-scale genome assembly reveals a highly dynamic effector repertoire of wheat powdery mildew. *New Phytol*. 2018: 221(4):2176–2189. https://doi.org/10.1111/nph.15529

Downloaded from https://academic.oup.com/plphys/article/197/4/kiaf067/8026087 by Bibliothek der RWTH Aachen user on 09 February 2026

Nielsen ME, Feechan A, Böhlenius H, Ueda T, Thordal-Christensen H. Arabidopsis ARF-GTP exchange factor, GNOM, mediates transport required for innate immunity and focal accumulation of syntaxin PEN1. *Proc Natl Acad Sci U S A*. 2012:109(28):11443–11448. https://doi.org/10.1073/pnas.1117596109

Nielsen ME, Jürgens G, Thordal-Christensen H. VPS9a activates the Rab5 GTPase ARA7 to confer distinct pre- and postinvasive plant innate immunity. *Plant Cell*. 2017:29(8):1927–1937. https://doi.org/10.1105/tpc.16.00859

Pedersen C, Ver Loren van Themaat E, McGuffin LJ, Abbott JC, Burgis TA, Barton G, Bindschedler LV, Lu X, Maekawa T, Weßling R, *et al.* Structure and evolution of barley powdery mildew effector candidates. *BMC Genomics*. 2012:13(1):694. https://doi.org/10.1186/1471-2164-13-694

Pennington HG, Jones R, Kwon S, Bonciani G, Thieron H, Chandler T, Luong P, Morgan SN, Przydacz M, Bozkurt T, *et al.* The fungal ribonuclease-like effector protein CSEP0064/BEC1054 represses plant immunity and interferes with degradation of host ribosomal RNA. *PLoS Pathog*. 2019:15(3):e1007620. https://doi.org/10.1371/journal.ppat.1007620

Peplowska K, Markgraf DF, Ostrowicz CW, Bange G, Ungermann C. The CORVET tethering complex interacts with the yeast Rab5 homolog Vps21 and is involved in endo-lysosomal biogenesis. *Dev Cell*. 2007:12(5):739–750. https://doi.org/10.1016/j.devcel.2007.03.006

Peterson MR, Emr SD. The class C Vps complex functions at multiple stages of the vacuolar transport pathway. *Traffic*. 2001:2(7):476–486. https://doi.org/10.1034/j.1600-0854.2001.20705.x

Petre B, Contreras MP, Bozkurt TO, Schattat MH, Sklenar J, Schornack S, Abd-El-Haliem A, Castells-Graells R, Lozano-Durán R, Dagdas YF, *et al.* Host-interactor screens of *Phytophthora infestans* RXLR proteins reveal vesicle trafficking as a major effector-targeted process. *Plant Cell*. 2021:33(5):1447–1471. https://doi.org/10.1093/plcell/koab069

Pliego C, Nowara D, Bonciani G, Gheorghe DM, Xu R, Surana P, Whigham E, Nettleton D, Bogdanove AJ, Wise RP, *et al.* Host-induced gene silencing in barley powdery mildew reveals a class of ribonuclease-like effectors. *Mol Plant Microbe Interact*. 2013:26(6):633–642. https://doi.org/10.1094/MPMI-01-13-0005-R

Qian J, Ibrahim HMM, Erz M, Kümmel F, Panstruga R, Kusch S. Long noncoding RNAs emerge from transposon-derived antisense sequences and may contribute to infection stage-specific transposon regulation in a fungal phytopathogen. *Mob DNA*. 2023:14(1):17. https://doi.org/10.1186/s13100-023-00305-6

Rieder SE, Emr SD. A novel RING finger protein complex essential for a late step in protein transport to the yeast vacuole. *Mol Biol Cell*. 1997:8(11):2307–2327. https://doi.org/10.1091/mbc.8.11.2307

Rink J, Ghigo E, Kalaidzidis Y, Zerial M. Rab conversion as a mechanism of progression from early to late endosomes. *Cell*. 2005:122(5):735–749. https://doi.org/10.1016/j.cell.2005.06.043

Robzyk K, Kassir Y. A simple and highly efficient procedure for rescuing autonomous plasmids from yeast. *Nucleic Acids Res*. 1992:20(14):3790. https://doi.org/10.1093/nar/20.14.3790

Rubiato HM, Liu M, O'Connell RJ, Nielsen ME. Plant SYP12 syntaxins mediate an evolutionarily conserved general immunity to filamentous pathogens. *eLife*. 2022:11:e73487. https://doi.org/10.7554/eLife.73487

Ruf A, Oberkofler L, Robatzek S, Weiberg A. Spotlight on plant RNA-containing extracellular vesicles. *Curr Opin Plant Biol*. 2022:69:102272. https://doi.org/10.1016/j.pbi.2022.102272

Schmidt SM, Kuhn H, Micali C, Liller C, Kwaaitaal M, Panstruga R. Interaction of a *Blumeria graminis* f. sp. *hordei* effector candidate with a barley ARF-GAP suggests that host vesicle trafficking is a fungal pathogenicity target. *Mol Plant Pathol*. 2014:15(6):535–549. https://doi.org/10.1111/mpp.12110

Schultz-Larsen T, Lenk A, Kalinowska K, Vestergaard LK, Pedersen C, Isono E, Thordal-Christensen H. The AMSH3 ESCRT-III-associated deubiquitinase is essential for plant immunity. *Cell Rep*. 2018:25(9):2329–2338.e5. https://doi.org/10.1016/j.celrep.2018.11.011

Seals DF, Eitzen G, Margolis N, Wickner WT, Price A. A Ypt/Rab effector complex containing the Sec1 homolog Vps33p is required for homotypic vacuole fusion. *Proc Natl Acad Sci U S A*. 2000:97(17):9402–9407. https://doi.org/10.1073/pnas.97.17.9402

Seeholzer S, Tsuchimatsu T, Jordan T, Bieri S, Pajonk S, Yang W, Jahoor A, Shimizu KK, Keller B, Schulze-Lefert P. Diversity at the *Mla* powdery mildew resistance locus from cultivated barley reveals sites of positive selection. *Mol Plant Microbe Interact*. 2010:23(4):497–509. https://doi.org/10.1094/MPMI-23-4-0497

Shang S, Liu G, Zhang S, Liang X, Zhang R, Sun G. A fungal CFEM-containing effector targets NPR1 regulator NIMIN2 to suppress plant immunity. *Plant Biotechnol J*. 2024:22(1):82–97. https://doi.org/10.1111/pbi.14166

Shvarev D, Schoppe J, König C, Perz A, Füllbrunn N, Kiontke S, Langemeyer L, Januliene D, Schnelle K, Kümmel D, *et al.* Structure of the HOPS tethering complex, a lysosomal membrane fusion machinery. *eLife*. 2022:11:e80901. https://doi.org/10.7554/eLife.80901

Sinclair R, Rosquete MR, Drakakaki G. Post-Golgi trafficking and transport of cell wall components. *Front Plant Sci*. 2018:9:1784. https://doi.org/10.3389/fpls.2018.01784

Sonah H, Zhang X, Deshmukh RK, Borhan MH, Fernando WGD, Belanger RR. Comparative transcriptomic analysis of virulence factors in *Leptosphaeria maculans* during compatible and incompatible interactions with canola. *Front Plant Sci*. 2016:7:1784. https://doi.org/10.3389/fpls.2016.01784

Spiller L, Manjula R, Leissing F, Basquin J, Bourilhon P, Sinitski D, Brandhofer M, Levecque S, Gerra S, Sabelleck B, *et al.* Plant MDL proteins synergize with the cytokine MIF at CXCR2 and CXCR4 receptors in human cells. *Sci Signal*. 2023:16(812):eadg2621. https://doi.org/10.1126/scisignal.adg2621

Takemoto K, Ebine K, Askani JC, Krüger F, Gonzalez ZA, Ito E, Goh T, Schumacher K, Nakano A, Ueda T. Distinct sets of tethering complexes, SNARE complexes, and Rab GTPases mediate membrane fusion at the vacuole in Arabidopsis. *Proc Natl Acad Sci U S A*. 2018:115(10):E2457–E2466. https://doi.org/10.1073/pnas.1717839115

Thomas WJ, Thireault CA, Kimbrel JA, Chang JH. Recombineering and stable integration of the *Pseudomonas syringae* pv. *syringae* 61 *hrp/hrc* cluster into the genome of the soil bacterium *Pseudomonas fluorescens* Pf0-1. *Plant J*. 2009:60(5):919–928. https://doi.org/10.1111/j.1365-313X.2009.03998.x

Thordal-Christensen H. A holistic view on plant effector-triggered immunity presented as an iceberg model. *Cell Mol Life Sci*. 2020:77(20):3963–3976. https://doi.org/10.1007/s00018-020-03515-w

Underwood W. The plant cell wall: a dynamic barrier against pathogen invasion. *Front Plant Sci*. 2012:3:85. https://doi.org/10.3389/fpls.2012.00085

Underwood W, Ryan A, Somerville SC. An Arabidopsis lipid flippase is required for timely recruitment of defenses to the host-pathogen interface at the plant cell surface. *Mol Plant*. 2017:10(6):805–820. https://doi.org/10.1016/j.molp.2017.04.003

Underwood W, Somerville SC. Focal accumulation of defences at sites of fungal pathogen attack. *J Exp Bot*. 2008:59(13):3501–3508. https://doi.org/10.1093/jxb/ern205

Downloaded from https://academic.oup.com/plphys/article/197/4/kiaf067/8026087 by Bibliothek der RWTH Aachen user on 09 February 2026

Vaghefi N, Kusch S, Németh MZ, Seress D, Braun U, Takamatsu S, Panstruga R, Kiss L. Beyond nuclear ribosomal DNA sequences: evolution, taxonomy, and closest known saprobic relatives of powdery mildew fungi (*Erysiphaceae*) inferred from their first comprehensive genome-scale phylogenetic analyses. *Front Microbiol*. 2022:13:903024. https://doi.org/10.3389/fmicb.2022.903024

van der Kant R, Jonker CTH, Wijdeven RH, Bakker J, Janssen L, Klumperman J, Neefjes J. Characterization of the mammalian CORVET and HOPS complexes and their modular restructuring for endosome specificity. *J Biol Chem*. 2015:290(51):30280–30290. https://doi.org/10.1074/jbc.M115.688440

von Bongartz K, Sabelleck B, Baquero Forero A, Kuhn H, Leissing F, Panstruga R. Comprehensive comparative assessment of the *Arabidopsis thaliana* MLO2-CALMODULIN2 interaction by various *in vitro* and *in vivo* protein-protein interaction assays. *Biochem J*. 2023:480(20):1615–1638. https://doi.org/10.1042/BCJ20230255

Wang D, Zhang D-D, Song J, Li J-J, Wang J, Li R, Klosterman SJ, Kong Z-Q, Lin F-Z, Dai X-F, *et al*. *Verticillium dahliae* CFEM proteins manipulate host immunity and differentially contribute to virulence. *BMC Biol*. 2022:20(1):55. https://doi.org/10.1186/s12915-022-01254-x

Wang J, Shine MB, Gao Q-M, Navarre D, Jiang W, Liu C, Chen Q, Hu G, Kachroo A. Enhanced disease susceptibility1 mediates pathogen resistance and virulence function of a bacterial effector in soybean. *Plant Physiol*. 2014:165(3):1269–1284. https://doi.org/10.1104/pp.114.242495

Wei D, Zhan W, Gao Y, Huang L, Gong R, Wang W, Zhang R, Wu Y, Gao S, Kang T. RAB31 marks and controls an ESCRT-independent exosome pathway. *Cell Res*. 2021:31(2):157–177. https://doi.org/10.1038/s41422-020-00409-1

Yuan H, Jin C, Pei H, Zhao L, Li X, Li J, Huang W, Fan R, Liu W, Shen Q-H. The powdery mildew effector CSEP0027 interacts with barley catalase to regulate host immunity. *Front Plant Sci*. 2021:12:733237. https://doi.org/10.3389/fpls.2021.733237

Yuen ELH, Shepherd S, Bozkurt TO. Traffic control: subversion of plant membrane trafficking by pathogens. *Annu Rev Phytopathol*. 2023:61(1):325–350. https://doi.org/10.1146/annurev-phyto-021622-123232

Zhang W-J, Pedersen C, Kwaaitaal M, Gregersen PL, Mørch SM, Hanisch S, Kristensen A, Fuglsang AT, Collinge DB, Thordal-Christensen H. Interaction of barley powdery mildew effector candidate CSEP0055 with the defence protein PR17c. *Mol Plant Pathol*. 2012:13(9):1110–1119. https://doi.org/10.1111/j.1364-3703.2012.00820.x

Zhu W, Wei W, Wu Y, Zhou Y, Peng F, Zhang S, Chen P, Xu X. BcCFEM1, a CFEM domain-containing protein with putative GPI-anchored site, is involved in pathogenicity, conidial production, and stress tolerance in *Botrytis cinerea*. *Front Microbiol*. 2017:8:1807. https://doi.org/10.3389/fmicb.2017.01807

Zuo N, Bai W-Z, Wei W-Q, Yuan T-L, Zhang D, Wang Y-Z, Tang W-H. Fungal CFEM effectors negatively regulate a maize wall-associated kinase by interacting with its alternatively spliced variant to dampen resistance. *Cell Rep*. 2022:41(13):111877. https://doi.org/10.1016/j.celrep.2022.111877

Downloaded from https://academic.oup.com/plphys/article/197/4/kiaf067/8026087 by Bibliothek der RWTH Aachen user on 09 February 2026